UNIVERSITY OF WISCONSIN
Cardiovascular Research Center

Cardiovascular Research Summit & Poster Fair

Focus on Heart Failure

December 2, 2021

Wisconsin Institute for Discovery
330 N. Orchard St.
Madison, WI

School of Medicine and Public Health
UNIVERSITY OF WISCONSIN–MADISON

SMPH CARDIOVASCULAR RESEARCH CENTER
27th Annual Scientific Poster Fair
Thursday, December 2, 2021

POSTER SUMMARY

Poster No.	Last Name	First Name	Department Affiliation	PI / Lab	Title
	Predocs				
1	**Aballo**	**Timothy**	Department of Cell & Regenerative Biology	Ge Lab	A Proteomics Perspective Of Cardiac Development In Swine Hearts
2	**Bayne**	**Elizabeth**	Department of Chemistry	Ge Lab	A Multi-Omics Strategy Enabled By Sequential Metabolomics And Proteomics For Human Pluripotent Stem Cell-Derived Cardiomyocytes
3	**Begeman**	**Ian**	Department of Cell & Regenerative Biology	Kang Lab	Dissecting Cardiac Regeneration Enhancers Dually Regulated By Activation And Repression
4	**Chapman**	**Emily**	Department of Chemistry	Ge Lab	Analysis of Sarcomeric Proteoforms In Ischemic Cardiomyopathy By Top-Down Proteomics
5	**Dangudubiyyam**	**Sri**	Department of Comparative Biosciences	Kumar Lab	Gestational Exposure Of Perfluorooctane Sulfonic Acid (PFOS) Increases Mean Arterial Pressure By Impaired Endothelium-Dependent Vasodilation And Heightened Vascular Contraction In Pregnant Rats
6	**Derrer**	**Megan**	Department of Pediatrics	Legare Lab	Heart Rate Variability Scores And Neurodevelopmental Outcome Following Neonatal Hypoxic-Ischemic Encephalopathy – Is There An Association?
7	**Dooge**	**Holly**	Department of Medicine	Valdivia Lab	Ablation Of Three Major Phosphorylation Sites In RyR2 Does Not Prevent Targeting Of The Channel By PKA And CaMKII
8	**El-Meanawy**	**Sarah**	Department of Medicine	Ramratnam Lab	Pharmacologic Inhibition Of Cardiac ROMK Does Not Worsen Myocardial Ischemia Reperfusion Injury But Prevents Further Protection From Ischemic Preconditioning
9	**Freel**	**Coleman**	Department of Obstetrics & Gynecology	Zheng Lab	TNFα Upregulates CXCL1, CXCL2, and CXCL3 in Vascular Endothelial Cells

Poster No.	Last Name	First Name	Department Affiliation	PI / Lab	Title
10	**Grindel**	**Samual**	Department of Medical Genetics	Ikeda Lab	Mice Overexpressing Tmem135 As A Model Of Cardiomyopathy With Metabolic Dysfunction
11	**Hiebing**	**Ashley**	Department of Biomedical Engineering	Witzenburg Lab	Computationally Modeling Cardiac Growth and Hemodynamics in Healthy Infants
12	**Jameson**	**Margaret**	Department of Neuroscience	Robertson Lab	Associated mRNAs Coordinate Biogenesis Of Functionally Related Ion Channels
13	**Kalluri**	**Manasa**	Department of Medicine	Eckhardt Lab	Electrophysiological Arrhythmia Characterization Of Stress-Induced Idiopathic VF iPS-CMs Using Fluorescent Optical Mapping
14	**Melby**	**Jake**	Department of Chemistry	Ge Lab	Patient-specific Human Induced Pluripotent Stem Cell-derived Engineered Cardiac Tissue Model Of Hypertrophic Cardiomyopathy
15	**Paltzer**	**Wyatt**	Department of Genetics	Mahmoud Lab	Elucidating the role of Mechanistic Target of Rapamycin Complex 1 during Heart Regeneration
16	**Patil**	**Vaidehi**	Department of Biomedical Engineering	Masters Lab	Valvular Endothelial Cells Regulate Lipid Infiltration in a Sex-Dependent Manner
17	**Reese**	**Kalina**	Department of Cell & Regenerative Biology	Ge Lab	Top-Down Mass Spectrometry Of Phospholamban Proteoforms Enabled By Photocleavable Surfactant
18	**Roberts**	**David**	Department of Chemistry	Ge Lab	Structural O-Glycoform Heterogeneity Analysis of the SARS-CoV-2 Spike Receptor Binding Domain for Rational Therapeutic Design to Treat COVID-19
19	**Rogers**	**Allison**	Cardiovascular Research, MOR Core	Hacker Lab	Using Novel 4D Strain Imaging To Characterize Murine Cardiac Phenotypes
20	**Salamon**	**Rebecca**	Department of Cell & Regenerative Biology	Mahoud Lab	Mapping Cardiac Innervation During Development, Disease, And Regeneration
21	**Stempien**	**Alana**	Department of Biomedical Engineering	Crone Lab	Enhanced Mechanical Function Of Cardiomyocytes Using Micropatterning And Co-Culture With Human iPSC-Derived Cardiac Fibroblasts
22	**Stevens**	**Christopher**	Department of Chemistry	Tang Lab	Synthesis of Mannose-6-Phosphonate Conjugate For Targeted Protein Degradation Through The Lysosome

Poster No.	Last Name	First Name	Department Affiliation	PI / Lab	Title
23	**Stevens-Sostre**	**Whitney**	Department of Neuroscience	Robertson Lab	Conformation Sensitive Antibody Reveals An Altered Cytosolic PAS/CNBh Assembly During hERG Channel Gating
24	**Tiambeng**	**Timothy**	Chemistry	Ge Lab	Native Mass Spectrometry of Human Cardiac Troponin Complexes Enabled By Functionalized Nanoparticle Enrichment And Online Size Exclusion Chromatography
25	**Turner**	**Daniel**	Department of Pharmacy	Glukhov Lab	Atrial-Like Engineered Cardiac Tissue as a Novel In Vitro Cardiac Model
26	**Han**	**Owen**	Department of Medicine	Glukhov Lab	Investigation of Anatomically Heterogeneous Transverse Axial Tubule System in Human Atrial Myocardium
27	**Zhang**	**Yanghai**	Department of Animal and Dairy Sciences	Guo Lab	RNA Binding Motif 20 (RBM20) Mutations and Phosphorylation In Cardiac Remodelling And Pathogenesis
28	**Zheng**	**Jingjing**	Department of Medicine	Valdivia Lab	RyR2 With Three Major Phosphorylation Sites Ablated Shows Blunted Luminal Ca^{2+} Sensitivity And Increased Early Afterdepolarization Susceptibility
	Postdocs				
29	**Bae**	**Jiyoung**	Department of Cell & Regenerative Biology	Mahmoud Lab	Carnitine Palmitoyltransferase (CPT) 1 Promotes Mammalian Heart Regeneration
30	**Brown**	**Kyle**	Department of Surgery	Gellman & Ge Lab	Proteomic Analysis of Functional Inward Rectifier Potassium Channel (Kir) 2.1 Reveals Several Novel Phosphorylation Sites
31	**Flores-Aldama**	**Lisandra**	Department of Neuroscience	Robertson Lab	A Hydrophobic Nexus At The Pas-Cap/Globular Pas/CNBHD Interface Tunes Deactiviation Kinetics Of Herg Channels
32	**Gregorich**	**Zachary**	Department of Medicine	Kamp Lab	Towards A Better Understanding Of The Function And Regulation Of LRRC10 In The Heart
33	**Hughey**	**Christina**	Department of Medicine	Stein Lab	Grayscale Ultrasound Texture Features Of Carotid And Brachial Arteries In People With HIV Infection Before And After Antiretroviral Therapy
34	**Knicklebine**	**Jennifer**	Department of Neuroscience	Robertson Lab	RNA Binding Proteins Associated With Translation Of hERG1a And 1b In The Heart

Poster No.	Last Name	First Name	Department Affiliation	PI / Lab	Title
35	**Lang**	**Di**	Department of Medicine	Glukhov Lab	Region-Specific Distribution Of Transversal-Axial Tubule System Organization Underlies Heterogeneity Of Calcium Dynamics In The Atrium
36	**Medvedev**	**Roman**	Department of Medicine	Glukhov Lab	Stretch-Induced Caveolae-Mediated Disruption Of cAMP Microdomains Leads To Arrhythmogenic Ca2+ Mishandling In Mouse Atrial Myocytes
37	**Mishra**	**Jay**	Department of Comparative Biosciences	Kumar Lab	Novel Role Of Compound 21, An Angiotensin Type 2 Receptor Agonist In Inducing Angiogenesis In Pregnant Human Uterine Artery Endothelial Cells
38	**Pewowaruk**	**Ryan**	Department of Medicine	Gepner Lab	Carotid Artery Stiffness Mechanisms Associated With Cardiovascular Disease Events And Incident Hypertension: The Multi-Ethnic Study of Atherosclerosis (MESA)
39	**Price**	**Tara**	Department of Biochemistry	Attie Lab	Role Of a/b-Hydrolase Domain 2 (ABHD2) In Lipid Metabolis
40	**Reilly**	**Louise**	Department of Medicine	Eckhardt Lab	I_{K1} and β-2 Adrenergic Response: Implications For Caveolar Membranes
41	**Rios-Perez**	**Erick**	Department of Neuroscience	Robertson Lab	Homeostatic Control of Cardiac Excitability By An RNA-Based Mechanism
42	**Roy**	**Sushmita**	Department of Medicine	Raval Lab	Human Cardiac Fibroblasts Transition To Myofibroblasts In *Vitro* And Differentially Express Angiogenic And Inflammatory Cytokines
43	**Solis**	**Christopher**	Department of Physiology and Biophysics	Russel Lab	Whole-Cell Mechanical Loading And Unloading Triggers More Post-Translational Modifications In Z-Disc Proteins Than Myosin Activators And Inhibitors
44	**Tattersall**	**Mathew**	Department of Medicine	Tattersall Lab	Persistent Asthma Is Associated With Carotid Plaque In The Multi-Ethnic Study Of Atherosclerosis (MESA)
45	**Veith**	**Alex**	Department of Oncology	Bradfield Lab	A Synthetic Biology Approach To Study Per-Arnt-Sim (PAS) Proteins In Cardiovascular Biology And Disease
46	**Wexuan**	**Cai**	Cardiovascular Research Center	Valdivia Lab	Molecular And Cellular Characterization Of RyR2 Mutations Linked to Long-QT Syndrome
47	**Wheeler**	**Nathan**	Department of Medicine	Dhingra Lab	Differences In Clinical Characteristics And Risk Of Death Between Recovered And Preserved Ejection Fraction

Poster No.	Last Name	First Name	Department Affiliation	PI / Lab	Title
48	**Zhang**	**Jianhua**	Department of Medicine	Kamp Lab	Heart Field-specific Lineages Differentiated from Human Pluripotent Stem Cells Generate Chamber-specific Cardiomyocytes for Disease Modeling and Cell Therapies
49	**Zhou**	**Tianhua (Tim)**	Department of Medicine	Raval Lab	Cultured Human Cardiac Myofibroblast's Expression of Sushi Containing Domain 2 Predicts the Assembly of Intact Fibronectin-Rich Extracellular Matrix

Poster #1

A Proteomics Perspective Of Cardiac Development In Swine Hearts

Timothy J. Aballo[1], Elizabeth F. Bayne[2], Wuqiang Zhu[3], Meng Zhao[3], Ahmed I. Mahmoud[1], Jianyi Zhang[3], Ying Ge[1,2]

Department of Cell and Regenerative Biology[1], Department of Chemistry[2], University of Wisconsin-Madison; Department of Biomedical Engineering[3], University of Alabama at Birmingham

Background: The neonatal swine heart possesses an endogenous ability to regenerate injured myocardium through the proliferation of pre-existing cardiomyocytes (CMs), but this regenerative capacity is lost shortly after birth. The molecular mechanisms governing the proliferative capacity of CMs during this early postnatal stage are unknown; therefore, there is great need to define the proteomic landscape during development to identify potential regulators of this regenerative process. Using an integrated top-down and bottom-up proteomics approach, we comprehensively characterized the molecular changes that occur throughout postnatal heart development to gain novel information about the regenerative window.

Methods: Left ventricular (LV) tissue was isolated from swine at postnatal days 1, 7, 28 and 56 (n=3). For bottom-up analysis, 1 mg LV tissue was homogenized in 0.2% Azo, and proteins were digested for 30 min with trypsin prior to reversed phase liquid chromatography (RPLC) interfaced with a trapped ion mobility spectrometer (TIMS) quadrupole time-of-flight (Q-TOF) mass spectrometer (Bruker timsTOF Pro). MSFragger and Perseus were used for bottom-up data analysis. For top-down analysis, myofilament proteins were enriched from 5 mg LV tissue using a differential pH extraction (HEPES, pH = 7.4 and TFA, pH = 2) and were analyzed by RPLC mass spectrometry (Bruker Q-TOF Impact II). Bruker DataAnalysis v4.3 and MASH Explorer were used for top-down data analysis.

Results and Discussion: We hypothesized there would be significant alterations in expression of proteins involved in cell cycle regulation, metabolism, and contraction. Bottom-up analysis of the global cardiac proteome provided insight into how a diverse array of cardiac proteins changed throughout development, while top-down analysis of myofilament protein extracts gave a “bird’s eye view” of myofilament composition, allowing for simultaneous quantification of protein expression levels and relative quantification of proteoforms, the functionally diverse protein species that arise from a single gene due to mRNA splicing and post-translation modifications (PTMs), at different stages of development in the swine heart.

Our global bottom-up proteomic analysis revealed distinct changes in proteins related to excitation-contraction coupling, cell cycle regulation, and metabolism. Specifically, we identified a shift in protein expression that supports oxidative phosphorylation over glycolysis, including an increase in subunits that make up succinate coenzyme A ligase, an enzyme involved in succinate production that has been shown to reduce cardiomyocyte proliferation.

With our top-down proteomics platform, we observed a transition of fetal sarcomeric isoforms to their adult counterparts. As sarcomere disassembly is uniquely observed during CM proliferation, th ese fetal isoforms may play an important role in this process during cardiac regeneration. Furthermore, while α-Tpm expression was consistent between all samples, the relative amount of phosphorylated α-Tpm decreased throughout the developmental window. This finding was consistent with a previous study that revealed a decrease in α-Tpm phosphorylation during the maturation human embryonic stem cell-derived cardiomyocytes.

Overall, we harnessed the power of global bottom-up proteomics and targeted top-down proteomics to provide a comprehensive view of how the swine heart proteome changes throughout development to guide future investigations into the molecular mechanisms associated with endogenous heart regeneration.

A Multi-omics Strategy Enabled By Sequential Metabolomics And Proteomics For Human Pluripotent Stem Cell-Derived Cardiomyocytes

Elizabeth F. Bayne[1], Aaron D. Simmons[2], David S. Roberts[1], Yanlong Zhu[3,4], Timothy J. Aballo[3,5], Benjamin Wancewicz[3], Sean P. Palecek[2], Ying Ge[1,3,4]

[1]*Department of Chemistry, University of Wisconsin-Madison, Madison, WI 53706, USA*
[2]*Department of Chemical and Biological Engineering, University of Wisconsin-Madison*
[3]*Department of Cell and Regenerative Biology, University of Wisconsin-Madison*
[4]*Human Proteomics Program, School of Medicine and Public Health, University of Wisconsin-Madison*
[5]*Molecular and Cellular Pharmacology Training Program, University of Wisconsin-Madison*

Background: Human pluripotent stem cell-derived cardiomyocytes (hPSC-CMs) show immense promise for use in precision medicine. However, hPSC-CMs in culture have not recapitulated the structural and functional properties of adult CMs *in vivo* thus far. To gain global insight into hPSC-CM biology, we introduce a multi-omics strategy for analyzing the hPSC-CM metabolome and proteome from the same cell culture, creating multi-dimensional profiles of hPSC-CMs. Here, we developed a sequential extraction method to capture metabolites and proteins from the same hPSC-CM monolayer culture and analyzed these extracts using high-resolution mass spectrometry (MS).

Methods: hPSCs were differentiated into cardiomyocytes using the GiWi protocol. A methanol-based quench was used to sequentially extract metabolites and proteins from hPSC-CMs. Metabolite-rich supernatant was directly infused into a Bruker 12T solarix Fourier Transform Ion Cylcotron Resonance MS using automated flow injection and electrospray ionization. Data were processed using MetaboScape v2021. Features were annotated using Mass Bank of North America and METLIN databases. The protein-rich cell pellet was resolubilized in a buffer containing MS-compatible surfactant Azo, enzymatically digested, and analyzed by LC-MS/MS using Bruker timsTOF Pro in Parallel Accumulation-Serial Fragmentation mode. Tandem mass spectra were searched against the UniProt human database using MaxQuant v1.6.17.0 (1% false discovery rate). Integrative pathway analysis was performed using MetaboAnalyst 5.0.

Results and Discussion: Our method achieves rapid, reproducible access to metabolites and proteins from a single monolayer of hPSC-CMs with excellent reproducibility. We annotated 205 metabolites/lipids and 4,008 proteins from 10^6 cells and created network profiles of molecular phenotypes of hPSC-CMs. We achieved broad coverage of metabolite classes including carbohydrates, amino acids, and a variety of phospholipid species. We identified metabolites important to hPSC-CM biology, including energy-yielding substrates such as glucose, ATP, fatty acids, acyl-carnitines, amino acids, and triglyceride (TAG) species.

We achieved consistent recovery of protein content from the residual cell pellet after initial metabolite extraction. Gene ontology analysis revealed highly diverse protein groups recovered from the sequentially-extracted hPSC-CM pellet, including strong representation of metabolic pathways, cardiac-specific pathways, and extracellular matrix proteins.

We integrated proteome and metabolome measurements to create network profiles of molecular phenotypes for hPSC-CMs. Out of 310 total pathways identified using metabolomics and proteomics data, 40 pathways were considered significantly overrepresented ($p \leq 0.05$). Highly populated pathways included those involved in protein synthesis (ribosome, spliceosome), ATP generation (oxidative phosphorylation), and cardiac muscle contraction. This multi-omics method achieves deep coverage of metabolites and proteins from a single well of hPSC-CMs, creating a multidimensional view of the hPSC-CM phenotype. This strategy can be used to generate biological hypotheses and identify biomarker candidates to advance the understanding of hPSC-CM biology.

Dissecting Cardiac Regeneration Enhancers Dually Regulated By Activation And Repression

Ian J. Begeman[1], Kwangdeok Shin[1], Daniel Osorio-Méndez[1], Andrew Kurth[1], Benjamin Emery[1], Trevor J. Chamberlain[2], Francisco J. Pelegri[2], Junsu Kang[1,3]

[1] Department of Cell and Regenerative Biology, School of Medicine and Public Health, University of Wisconsin–Madison
[2] Laboratory of Genetics, University of Wisconsin–Madison
[3] UW Carbone Cancer Center, School of Medicine and Public Health, University of Wisconsin–Madison

Heart regeneration in regeneration-competent organisms can be accomplished through remodeling gene expression in response to cardiac injury. This dynamic transcriptional response relies on the activities of tissue regeneration enhancer elements (TREEs). However, the mechanisms underlying TREEs are poorly understood. We dissected a cardiac regeneration enhancer in zebrafish to elucidate the mechanisms governing spatiotemporal gene expression during heart regeneration. *Cardiac leptin b regeneration enhancer* (*cLEN*) exhibits dynamic, regeneration-dependent activity in the heart. We found that multiple injury-activated regulatory elements are distributed throughout the enhancer region. This analysis also revealed that cardiac regeneration enhancers are not only activated by injury, but surprisingly are also actively repressed in the absence of injury. Our studies identified a short 22-bp DNA element containing a key repressive element. Comparative analysis across *Danio* species indicated that the repressive element is conserved in closely related species. By analyzing sequence similarity to the *cLEN* repressive element, evolution conservation, epigenomic and transcriptomic profiles of uninjured and regenerating hearts, and candidate target gene function, we have identified candidate cardiac regeneration enhancers in the genomes of zebrafish, mice, and humans that may also be dually regulated by activation and repression. Using transgenic assays, we demonstrated cardiac regeneration-dependent activation of multiple candidate enhancers. Incorporating both activation and repression components into the mechanism of tissue regeneration constitutes a new paradigm that may be extrapolated to other regeneration scenarios. Further, by identifying additional dually regulated regeneration enhancers, we may improve our understanding of transcriptional mechanisms underlying heart regeneration, build gene regulatory networks, and identify potential targets for improving heart repair.

Analysis Of Sarcomeric Proteoforms In Ischemic Cardiomyopathy By Top-Down Proteomics

Emily A. Chapman[1], Elizabeth F. Bayne[1], Timothy N. Tiambeng[1], Jake A. Melby[1], Tianhua Zhou[2], Ying Ge[1,3,4]

[1]Depart. Of Chemistry, University of Wisconsin - Madison
[2]Depart. of Medicine, University of Wisconsin - Madison
[3]Depart. of Cell and Regenerative Biology, University of Wisconsin – Madison
[4]Human Proteomics Program, University of Wisconsin - Madison

Background: Heart failure is the leading cause of mortality worldwide. Ischemic cardiomyopathy (ICM) is a prominent form of heart failure wherein left ventricular (LV) systolic dysfunction reduces blood flow to the heart, leading to oxygen deprivation and inducing myocardial hypoxia. While heart failure is largely associated with significant changes to the myocardium at a cellular and molecular level, the role of sarcomeric post-translational modifications (PTMs) and alternative splicing of RNA in ICM etiology remains undefined. Thus, we studied cardiac tissues from patients in end-stage ischemic heart failure to uncover changes in the cardiac proteome. We have implemented mass spectrometry (MS)-based top-down proteomics to quantify sarcomeric PTMs and isoform expression to reveal the molecular changes correlated to left ventricular dysfunction in ICM patients.

Methods: Human cardiac tissue from failing ICM hearts was collected during left ventricular assist device implantation and compared to non-failing donor hearts (n=16 for each group). Tissues were snap-frozen in liquid nitrogen until further analysis. Sarcomeric proteins were enriched from flash-frozen tissue using a differential pH-based extraction (HEPES, pH=7.4 and TFA, pH=2). Proteins were separated by online reverse-phase liquid chromatography (LC). MS data were acquired using a Bruker maXis II quadrupole time of flight mass spectrometer. Data analysis was performed using Bruker DataAnalysis v. 4.3 and MASH Explorer. To quantify protein expression across samples, the top 5 most abundant ions of each proteoform within the same protein family were selected to create extracted ion chromatograms.

Results & Discussion: We have implemented label-free quantitative top-down proteomics to analyze human cardiac tissues from failing ICM and non-failing donor hearts (n=16 for each). We isotopically resolved key sarcomere proteins ranging from 16 to 42 kDa within 5 ppm mass error from the human tissue extracts. To quantitate sarcomeric isoforms, we evaluated the linearity of MS signal in relation to amount of total protein injected. A mutual linear range was established for key sarcomeric proteins by measuring the areas under the curve after integrating extracted ion chromatograms for proteoform families. Next, we quantitated sarcomeric PTMs and isoform expression in ICM compared to non-failing donor samples. Phosphorylation peaks with mass shifts of 80 Da were quantitated to compare the phosphorylation levels between the ICM and non-failing donor groups. Notably, we observed a significant decrease in the mono-phosphorylated (*p*cTnI) and bis-phosphorylated (*pp*cTnI) proteoforms of cTnI in ICM hearts compared to donor hearts, with *p*cTnI decreasing from 55% in non-ICM hearts to 25% in ICM hearts and *pp*cTnI decreasing from 20% to 4%. Additionally, we observed a significant decrease in the mono-phosphorylated form of Z-disc protein ENH2, with *p*ENH2 decreasing from 65% to 30%. Overall, these results uncover molecular changes to important contractile proteins during ischemic heart failure, thus elucidating molecular mechanisms underlying ICM.

Gestational Exposure Of Perfluorooctane Sulfonic Acid (PFOS) Increases Mean Arterial Pressure By Impaired Endothelium-Dependent Vasodilation And Heightened Vascular Contraction In Pregnant Rats

Sri Vidya Dangudubiyyam[1], Jay S. Mishra[1], Ruolin Song[1] and Sathish Kumar[1]

[1]*Department of Comparative Biosciences*

Background: Pregnancy is associated with adaptive hemodynamic and vascular changes such as enhanced vasodilation, decreased blood pressure, and increased uterine artery blood flow. In contrast, preeclampsia is associated with hypertension and abnormal vascular function. The cause for this abnormal vascular function in preeclampsia remains unclear. Eight out of nine epidemiological studies show that plasma perfluorooctane sulfonic acid (PFOS), a persistent environmental pollutant, is elevated in pregnant women with hypertensive pregnancy disorders. Hence we hypothesized that PFOS exposure during pregnancy impairs gestational vascular adaptations via impaired endothelium-dependent vasodilation and heightened angiotensin II-mediated vascular contraction.

Methods: Pregnant Sprague-Dawley rats were administered with PFOS (50 µg/mL; n=7) through drinking water from gestational day (GD) 4 until term (GD20). Controls (n=7) received standard deionized waters with no detectable PFOS. Blood pressures were assessed using a non-invasive CODA tail-cuff system, and cardiac function and uterine artery blood flow were determined using Doppler ultrasound. Uterine artery vascular reactivity was assessed with a wire myograph. Total eNOS and AT1R and AT2R mRNA expression and protein levels were also examined in uterine arteries. Placental and fetal weights were also measured.

Results: Mean arterial pressures were significantly higher at GD 18 to GD 20 in PFOS-exposed dams compared to controls. Uterine artery blood flow was reduced in PFOS dams. Echocardiographic measurements showed a significant increase in ejection fraction and fractional shortening and increased left ventricular anterior and posterior wall thickness at end-systole in PFOS dams. Endothelium-dependent relaxation responses to acetylcholine were significantly lower, while endothelium-independent contraction to angiotensin II was increased in PFOS dams compared to controls. AT1aR mRNA expression was increased while AT1bR mRNA and AT1R protein expression did not change. AT2R and eNOS mRNA and protein expression were decreased in PFOS dams. Placental weights (control: 0.54 ± 0.01 g; PFOS-exposed: 0.49 ± 0.01 g) and fetal weights (control: 4.09 ± 0.14 g; PFOS-exposed: 3.56 ± 0.09 g) were significantly decreased in PFOS dams compared to controls.

Discussion: Elevated maternal PFOS caused hypertension, cardiac hypertrophy and decreased in uterine blood flow through blunting of endothelium-dependent vasodilation and exacerbation of angiotensin II induced contractions, providing a molecular mechanism linking maternal PFOS exposure and preeclampsia.

Heart Rate Variability Scores And Neurodevelopmental Outcome Following Neonatal Hypoxic-ischemic Encephalopathy – Is There An Association?

Megan A Derrer[1], Janet M Legare[2]

[1]*Department of Pediatrics, Division of Neonatology*
[2]*Department of Pediatrics, Division of Developmental Pediatrics and Rehab Medicine*

Background: Monitoring of fetal heartrate variability has been used to assess for signs of intolerance of labor and concern for perinatal asphyxia by obstetricians for decades. Heart rate variability monitoring software (HeRO monitoring) has been found to be predictive of sepsis and necrotizing enterocolitis in very low birth weight and extremely low birth weight infants. At AFCH, the NICU has HeRO monitoring equipment that is used on every baby, most of whom are late preterm or term infants with surgical needs or neurological concerns such as HIE. The standard of care for infants with moderate to severe HIE is therapeutic hypothermia. The purpose of this study is to determine if there is any association between HeRO scores and neurodevelopmental outcome of full term infants diagnosed with HIE, as well as to begin to establish expected patterns of HeRO score variability in our small patient population.

Methods: The EMR of infants admitted to AFCH NICU with a diagnosis of neonatal encephalopathy from the opening of the unit in May 2014 through March 1, 2021 were reviewed. Exclusion criteria included documentation that hypoxia was unlikely cause of encephalopathy, genetic disorders, and multiple congenital anomalies, and infants that were cooled at other facilities. Collection of maternal medical and pregnancy complications, maternal medications, gestational age, gender, ethnicity, mode of delivery, Apgar scores, chest compressions at delivery, cord or first infant blood gases, severity of HIE, any procedures performed, infant and cooling blanket temperatures, HeRO scores, subsequent infant blood gases and lactate levels, sedative medication received, cumulative dose of sedation medication, antiepileptic medications given, head imaging results were collected. Follow up data regarding whether patients were below average, average, or above average on developmental assessments in addition to documented concerns expressed by parents or developmental pediatricians at Waisman Center Newborn Follow Up Clinic was also collected. Data analysis is currently ongoing, but HeRO scores between patients who were not cooled because of contraindications, and those diagnosed with mild, moderate, and severe HIE who underwent cooling will be compared. Imaging results and developmental assessments will also be compared related to HeRO scores.

Results/Discussion: Data analysis is ongoing at this time. There were 73 patients identified with a diagnosis of encephalopathy, 46 met inclusion criteria. 27/46 (59%) received chest compressions at delivery. 6 infants died. Of the survivors, 33/40 (83%) had at least one developmental follow up visit. Data collected from admission was limited by completeness of documentation, and developmental assessment data was affected by variation in assessments used. Developmental data is still being collected due to upcoming appointments.

HeRO monitoring has mostly been studied in very or extremely low birth weight infants as a predictor of sepsis, but with increasing data in other populations, such as those with HIE, it may be helpful for prognostication and helping determine which infants are at risk of adverse outcomes. Data is not yet fully analyzed, however the patterns that can be established by graphing HeRO scores against time throughout admission, especially during cooling and rewarming, may be useful in demonstrating patients who are falling outside of the expected ranges and should be further evaluated for infection. The data may also be helpful for beginning to establish expected ranges of HeRO scores for different sedative, analgesic, and paralytic medications. An unexpected result of this study was the number of infants who received chest compressions, which provides an opportunity for outreach and further education on resuscitation. Limitations include small sample size, incompleteness of documentation and variation in developmental assessments, which offers opportunity for further QI projects to improve documentation and standardize longitudinal care of these complex infants.

Ablation Of Three Major Phosphorylation Sites In RyR2 Does Not Prevent Targeting Of The Channel By PKA And CaMKII

Holly C. Dooge, Héctor H. Valdivia, Francisco J. Alvarado

Department of Medicine and Cardiovascular Research Center, University of Wisconsin-Madison School of Medicine and Public Health, Madison, Wisconsin.

Background: Ryanodine Receptor 2 (RyR2) plays a critical role in cardiac excitation-contraction coupling by allowing the calcium (Ca^{2+}) necessary for contraction to leave its store in the sarcoplasmic reticulum (SR) and flood the cytoplasm of cardiomyocytes. During the fight-or-flight response, β-adrenergic stimulation enhances calcium cycling in the ventricles, leading to increased heart contractility and rate of relaxation. Many calcium handling proteins are regulated downstream of β-adrenergic signaling through phosphorylation by Protein Kinase A (PKA) or Ca^{2+}/calmodulin-dependent Protein Kinase II (CaMKII). While RyR2 is one such protein, the physiological effects of its interaction with these kinases during the adrenergic response are still unknown. We generated a mouse model in which the three major phosphorylation sites in RyR2 are substituted by the non-phosphorylatable residue alanine (RyR2-S2030A/S2808A/S2814A, triple phospho-mutant or TPM). We then used ^{32}P incorporation assays to determine the extent to which TPM channels are phosphorylated by PKA and CaMKII in vitro.

Methods: The TPM mouse model was generated at the Biotechnology Center Genome Editing and Animal Models Facility using CRISPR/Cas9 technology. The correct location of the three mutations was validated using Sanger sequencing and western blots with phospho-specific antibodies. RyR2 channels were immunoprecipitated from cardiac microsomes prepared from WT and TPM mice. Samples were then phosphorylated with PKA or CaMKII in the presence of [γ-^{32}P]ATP. Western blotting and phosphor imaging were implemented to detect phosphorylation at key sites and the incorporation of radioactive phosphates (^{32}P) respectively.

Results: Total expression of RyR2 measured using western blots was comparable between WT and TPM hearts (100.0±5.7% vs 105.5±10.3%, respectively; $p = 0.6440$, t-test), while no phosphorylation of S2030, S2808 or S2814 was detectable in TPM hearts. Treatment of WT samples with PKA produces robust phosphorylation of S2030 and S2808, while CaMKII phosphorylated prominently S2808 and S2814. As expected, we did not observe changes in TPM samples. Incorporation of ^{32}P by PKA was lower in TPM samples compared to WT controls (100.0±5.0% vs. 68.0±7.5%; $p = 0.0071$, t-test). Remarkably, CaMKII produced similar incorporation of ^{32}P for both WT and TPM microsomes. We are in the process of quantifying the extent to which CaMKII phosphorylates TPM channels.

Conclusion: Overall, our data suggest that RyR2 contains residues that can be targeted by both CaMKII and PKA in addition to the three sites widely studied in the literature. The potential for multiple additional CaMKII sites is remarkable, given that both WT and TPM samples had similar levels of ^{32}P incorporation. The TPM mouse model has allowed us to look beyond the three major RyR2 phospho-sites. Further research is now necessary to evaluate the β-adrenergic response in TPM hearts and evaluation the physiological relevance of RyR2 phosphorylation.

Pharmacologic Inhibition Of Cardiac ROMK Does Not Worsen Myocardial Ischemia-Reperfusion Injury But Prevents Further Protection From Ischemic Preconditioning.

Sarah El-Meanawy[1], Holly Dooge[1], Francisco J. Alvarado[1], Jonathan Makielski[1], Jack Kyle[1], Mohun Ramratnam[1]

[1]*University of Wisconsin, Department of Medicine, Division of Cardiology*

Background: Activation of potassium channels in cardiac mitochondria promote cardio-protection after acute cardiovascular stress. The recently discovered renal outer medullary potassium channel (ROMK) in cardiac mitochondria was shown to be involved in cellular cytoprotection *in vitro* but constitutive cardiac knockout of ROMK in mice did not mediate ischemia-reperfusion (IR) injury or affect cardio-protection from ischemic preconditioning (IPC). In this investigation we pharmacologically (compound A, MERCK) inhibit the cardiac ROMK channel to test whether acute block would affect IR injury or alter mitochondrial membrane potential.

Methods: Hearts from C57BL/6J male WT mice were subjected to an *ex vivo* ischemia (45 minutes)-reperfusion (60 minutes) injury protocol with or without IPC (3 cycles of 3 minutes of ischemia). Mouse hearts were perfused with a modified Krebs-Henseleit buffer with vehicle or compound A throughout the protocol. A fluid filled balloon catheter was placed in the left ventricle for hemodynamic monitoring. At the end of the protocol, hearts were sectioned and stained with TTC to quantify infarct size. To measure mitochondrial membrane potential ($\Delta\psi m$), isolated cardiomyocytes from male WT hearts treated with or without compound A were stained with TMRE for 30 minutes and imaged with a confocal microscope during perfusion with FCCP.

Results: WT male mouse hearts perfused with compound A demonstrated an unexpected trend towards improved left ventricular developed pressure (LVDP) recovery (53% ± 8% vs 64% ± 13%, P =0.14, N=4-5/group) and infarct size (42% ± 9% vs. 56% ± 8%, P = 0.15, N=4-5/group) after IR injury compared to vehicle perfused hearts. In addition, WT mouse hearts perfused with vehicle were protected from IR injury after an IPC stimulus (infract size: 56% ± 8% vs 31% ± 3%, P = 0.009, N = 5/group). In contrast, hearts perfused with compound A did not demonstrate improvement in IR injury when given a preconditioning stimulus (LVDP; 64% ± 13% vs 67% ± 3% P =0.47; infract size; 42% ± 9% vs. 47% ± 11%, P= 0.37 N=4/5 per group). In another set of experiments, isolated cardiomyocytes from WT mice treated with compound A had increased resting mitochondrial membrane potential compared to untreated isolated cardiomyocytes (11 ± 5 au vs. 30 ± 5 au, P=0.016, N=2).

Conclusion: Our study demonstrates that acute pharmacologic inhibition of ROMK does not worsen IR injury but may reduce cardio-protection from ischemic preconditioning. This may occur by increasing mitochondrial membrane potential and preventing mitochondrial uncoupling. While prior studies using mice with constitutive cardiac specific deletion of ROMK did not show a relationship with IR injury or IPC, further research in conditional KO ROMK models may elucidate whether ROMK plays a role in ischemic preconditioning versus off target effects that could be a reason for our findings. Nevertheless, further research to understand the significance of cardiac ROMK is needed to promote the clinical utility of ROMK inhibitors for hypertension.

TNFα Upregulates CXCL1, CXCL2, And CXCL3 In Vascular Endothelial Cells

Colman Freel[1], Ying-jie Zhao[1], Alex Uy[1], Chi Zhou[2], Jing Zheng[1]

[1]Department of Obstetrics and Gynecology, School of Medicine and Public Health, University of Wisconsin—Madison
[2] Department of Obstetrics and Gynecology, College of Medicine, University of Arizona—Tucson

Background: Cardiovascular diseases (CVDs) remain a leading cause of death globally. The complex etiology of CVDs dictates that special attention be paid to the molecular mechanisms underlying vascular function, particularly within the endothelium, which is markedly impaired in CVDs. Tumor Necrosis Factor-Alpha (TNFα) is a pro-inflammatory cytokine and a key regulator of endothelial function that is upregulated in CVDs. Downstream targets of TNFα, CXCL1, CXCL2, and CXCL3, are chemotactic cytokines primarily responsible for leukocyte recruitment during inflammation and are similarly associated with CVDs (e.g., atherosclerosis and stroke). Despite the general characterization of TNFα on CXC chemokine expression, many regulatory effects have not been explored in Human Umbilical Vein Endothelial Cells (HUVECs), a widely used model of endothelial cells and critical tool in CVD research. Given their potential to critically regulate endothelial function, we sought to characterize the regulation of CXCL1, CXCL2, and CXCL3 within the TNFα signaling pathway.

Methods: To investigate the roles of TNFα on CXCL2 and CXCL3, we performed a timed dose-response test examining CXCL2 and CXCL3 mRNA expression in pooled HUVECs using RT-qPCR. We followed our test with RT-qPCR analysis of CXCL1, CXCL2, and CXCL3 in independent HUVEC preparations dosed with 10ng/mL TNFα for 24 hours. We confirmed the upregulation of CXCL2 synthesis *in vitro* by performing an ELISA of the cell culture supernatants.

Results: TNFα increased CXCL2 and CXCL3 mRNA expression in a time- and dose-dependent manner but appeared to weaken culture monolayers. TNFα significantly upregulated CXCL1, CXCL2, and CXCL3 mRNA expression between 5- and 6-fold in HUVEC preparations. In addition, our ELISA results indicated CXCL2 mRNA upregulation was translated to cytokine synthesis *in vitro*.

Discussion: Our study effectively demonstrates that TNFα is an upstream upregulator of CXCL1, CXCL2, and CXCL3 in HUVECs. Furthermore, the apparent weakening of culture monolayers in our timed dose-response tests indicates CXCL2 and CXCL3 may be crucial intermediary signaling molecules in TNFα's regulation of endothelial function, but further studies are necessary to examine the effects of CXC chemokines on specific endothelial cell functions.

Mice Overexpressing *Tmem135* As A Model Of Cardiomyopathy With Metabolic Dysfunction

Samuel Grindel[1], Michael Landowski[1,2], Sakae Ikeda[1,2], Timothy J. Kamp[3,4], Akihiro Ikeda[1,2]

[1]Medical Genetics, University of Wisconsin-Madison, Madison, WI, United States
[2]McPherson Eye Research Institute, University of Wisconsin-Madison, Madison, WI, United States
[3]Cellular and Molecular Arrhythmia Research Program, Division of Cardiovascular Medicine, Department of Medicine, University of Wisconsin-Madison, WI, United States
[4]Department of Cell and Regenerative Biology, University of Wisconsin-Madison, WI, United States

Background: Overexpression of *Tmem135* (*Tmem135* TG) induces cardiac pathologies such as mitochondrial fragmentation, cardiac hypertrophy, and interstitial fibrosis in mice. *Tmem135* TG cardiac phenotypes were highly variable, possibly due to a mixed background of C57BL/6J and FVB/NJ. Here, we generated *Tmem135* TG mice on a congenic FVB/NJ (FVB) background (FVB-TG), and observed juvenile death between the ages of postnatal day (P) 20 and P35 in 58.5% of FVB-TG mice. We hypothesized that juvenile death in FVB-TG mice is due to cardiac dysfunction, therefore this study aims to characterize the cardiac phenotype of FVB-TG mice during this critical period.

Methods: Male and female FVB-TG mice and wild-type (WT) littermates between the ages P20 and P30 were used. Cardiac function was assessed through electrocardiogram (ECG) and echocardiogram (echo). Gene expression analysis was performed by RNA-sequencing of whole heart homogenates. Protein analysis of whole heart lysates was performed through western blotting. Hearts were collected for ultrastructural, histological, and immunofluorescent assessment. We also tested the effect of ketone body supplementation on cardiac phenotypes.

Results: Functional assessment of FVB-TG hearts at P25 by ECG and echo revealed atrial flutter and left ventricular hypertrophy (LVH), respectively. Increased heart to body weight ratio by P25 supports LVH finding in FVB-TG mice. Histological analysis showed drastic changes in FVB-TG hearts throughout the critical period. By P20, extensive cardiomyocyte degeneration exists. Degenerative changes were significantly reduced by P30 suggestive of cardiac remodeling during this period. We observed a significant increase in interstitial fibrosis by P30, consistent with cardiac dysfunction and remodeling. To assess the molecular basis of these histological alterations, a gene expression analysis was performed at P25. An upregulation of extracellular matrix, fibroblast, and macrophage genes supported observed cardiac remodeling, while a downregulation of contraction element and ion channel genes supported cardiac dysfunction. Gene expression analysis also indicated altered metabolic regulation with downregulation of lipid metabolism and mitochondrial genes corresponding with an upregulation in genes involved in glucose metabolism. Additionally, FVB-TG hearts have decreased beta-oxidation, oxidative phosphorylation, mitochondria, and peroxisome proteins by P30 consistent with alterations in gene expression. Finally, ketone body supplementation rescued juvenile death and cardiac vacuolization.

Discussion: FVB-TG mice experience high rates of juvenile death between P20 and P35. Functional and histological analyses point towards cardiomyopathy as the cause of death. An adult murine heart relies heavily on lipid metabolism to supply its vast energy demands. FVB-TG mice show peroxisome and mitochondria dysfunction, organelles central to lipid metabolism. FVB-TG hearts decrease lipid metabolism and potentially increase their reliance on glucose as a metabolic substrate, a common feature of heart failure pathogenesis. Since ketone bodies can be an alternative source of acetyl-CoA for the tricarboxylic acid cycle and subsequent oxidative phosphorylation, they may allow FVB-TG hearts to bypass the need for beta-oxidation to fuel mitochondria. This study highlights the pathogenic effect of *Tmem135* overexpression on the heart. FVB-TG mice can serve as a unique model to study the molecular mechanisms underlying cardiomyopathy due to metabolic dysregulation.

Poster #11

Computationally Modeling Cardiac Growth And Hemodynamics In Healthy Infants

Ashley Hiebing[1], Riley Pieper[1], Colleen Witzenburg[1]

[1]*Department of Biomedical Engineering, University of Wisconsin-Madison*

Background: Previous computer models have successfully predicted cardiac growth and remodeling in adults with various pathologies, including hypertension, valvular disease, and myocardial infarction. Applying these models to infants and children is complicated by the fact that they also undergo normal, somatic cardiac growth and remodeling.

Our objective was to create a computational model to predict ventricular dimensions and hemodynamics in healthy, growing infants.

Methods: A left ventricular growth model previously published by our lab for adult canines was modified for healthy infants. The four heart chambers were modeled as time-varying elastances coupled to a circuit model of the circulation. Circulation parameters were allometrically scaled for human infants. Early trends in systemic and pulmonary vascular resistance were fit to clinical data rather than scaled due to the dramatic reduction in pulmonary vascular resistance and marked increase in overall systemic vascular resistance immediately post-birth. Ventricular growth was driven by perturbations in myocyte strain, a non-dimensional metric. Reported heart rate was input directly into the model.

Results: The model successfully matched clinically measured values of systemic and pulmonary pressures, end-systolic and end-diastolic left and right ventricular volumes, maximum atrial volumes, and left ventricular end-diastolic thickness within one standard deviation of multiple studies for children aged 0-3 years (Figure). LV end-systolic and right ventricular end-diastolic thicknesses followed clinical trends but were outside of established ranges.

Discussion: Our model predicts hemodynamics and ventricular dimensions for healthy children from birth to 3 years. From this, we can gain a greater understanding of the interplay between somatic and pathological growth in infants and children with congenital heart defects

Poster #12

Associated mRNAs Coordinate Biogenesis Of Functionally Related Ion Channels

Margaret B. Jameson[1], Catherine A. Eichel[1], Erick B. Rios-Perez[1], Fang Liu[1], Avtar S. Roopra[1] and Gail A. Robertson[1]

[1]*Department of Neuroscience, University of Wisconsin-Madison, Madison, WI*

Background: Expression of ion channels underlying the heart's rhythmic beating must be precisely coordinated to fulfill their physiological roles and protect the heart from arrhythmias. How cells determine proper ratios of different ion channels mediating repolarization, the most vulnerable phase of the ventricular action potential, is poorly understood. Here, we tested the hypothesis that transcripts encoding ion channels necessary for repolarization are cotranslationally associated and regulated.

Methods: We assayed transcript association using multiple approaches. We performed correlation analysis of publicly available RNAseq databases of transcriptome data. We visualized mRNA transcripts using single-molecule fluorescence in-situ hybridization (smFISH), employing short, singly labeled antisense oligonucleotide probes incorporating bright organic dyes. The resulting signals provided quantitative measurements in three dimensions as imaged and analyzed using FISH-QUANT and Matlab software, including measurements of colocalization at distances close to the diffraction limit of light. A second approach revealing mRNA association is shRNA knockdown, which reduces transcripts encoding functionally related proteins by an as-yet unknown mechanism. The resulting “co-knockdown” effect was assayed using RT-PCR and electrophysiology of the encoded ion channels.

Results: Analysis of publicly available RNAseq databases revealed *hERG1a* transcripts are positively correlated with other ion channels, namely *SCN5A, CACNA1C, KCNQ1,* and *KCND2/3* in heart (R=0.91-0.96), but not, e.g., adipose tissue (-0.58-0.26). Similar pairwise correlations in numbers of mRNA molecules occurred in individual iPSCs as revealed by smFISH. The mRNA molecules colocalized to a degree greater than that expected by chance (8-12% vs. 3%), and the colocalization was strikingly enriched by approximately four-fold in *hERG1a* translational complexes. Within the limits of four-color detection, translating *hERG1a* preferentially associated with one mRNA molecule rather than two (or, presumably, more). Importantly, the associated mRNA molecule was found to simultaneously undergo translation. Specific silencing of either *hERG1a* or *hERG1b* transcripts concomitantly reduced expression of associated transcripts as determined by qPCR in a manner not attributable to off-target effects. Patch-clamp electrophysiology in cardiomyocytes derived from human iPSCs revealed a corresponding reduction in I_{Kr}, I_{Na}, $I_{Na,late}$, $I_{Ca,L,}$ and I_{Ks} currents following *hERG1b* (or *hERG1a*) mRNA silencing, indicating the mRNAs affected by knockdown were those undergoing translation and not sequestered for degradation.

Discussion: These results reveal a novel mechanism by which ion channels producing the cardiac action potential are co-synthesized from heterotypic pairs of associated mRNA molecules. We speculate co-biosynthesis helps establish the balance of ion channel expression required for a stable action potential while co-knockdown unmasks the paired mRNA partner and accelerates its degradation, mitigating the risk for arrhythmias.

Poster #13

Electrophysiological Arrhythmia Characterization Of Stress-Induced Idiopathic VF iPS-CMs Using Fluorescent Optical Mapping

Manasa Kalluri[1], Di Lang, Ph.D.[1], Corey L. Anderson, Ph.D.[1], Alexey V. Glukhov, Ph.D. [1], Louise Reilly, Ph.D.[1], Lee L. Eckhardt, M.D.[1]

[1]Cellular and Molecular Arrhythmia Research Program, University of Wisconsin School of Medicine and Public Health, Madison WI

Background: Idiopathic ventricular fibrillation (IVF) is a clinically challenging disease entity, as phenotypic characteristics are lacking. We studied induced pluripotent stem cell-derived cardiomyocytes (iPS-CMs) from a patient with stress-induced IVF to better understand the cellular arrhythmia mechanism.

Methods: iPS-CMs were generated from control (WT) and stress-induced IVF (si-IVF) patient-specific iPSC lines. Calcium-mediated electrophysiological responses were monitored in both cell lines via high-speed fluorescent single-cell optical mapping imaging techniques using calcium-sensitive dye (Fluo-4 AM) and application of electrical pacing (0.5Hz) before and after 1 x 10^{-6} mM isoproterenol (ISO)). The experiment was conducted as a blind study with respect to cell type, unblinded after data analysis. Statistical analysis was conducted using Sidak's multiple comparisons test.

Results: Ca^{2+} transient (CaT) duration and rise time were compared between WT and si-IVF cells. si-IVF cells had a longer CaT rise time (ms) at baseline (BSL) ($p<0.05$) (86+/- 5.45, n=54) and after ISO (83.88 +/- 5.12, n=41) than WT cells (BSL: 64.5 +/- 3.72, n=40) (ISO: 72+/- 9.92, n=10) ($p<0.05$). si-IVF cells had a shorter CaT duration (ms) at BSL (1,069 +/- 36.00, n=54) than WT cells at BSL (1,280 +/- 37.59, n=40) ($p<0.05$), with no significant difference after ISO (IVF: 1,073 +/- 44.51, n=41 and WT: 1,230 +/- 32.79, n=10) ($p>0.05$). Further, following administration of ISO, 11.5% of the si-IVF cells exhibited arrhythmic behavior with rapid continuous spontaneous Ca2+ release, compared to 0.0% of WT cells.

Discussion: We demonstrate the feasibility of differentiating iPS-CMs from patients while investigating the arrhythmogenicity of si-IVF cells compared to controls using optical mapping. Insights from CaT duration, rise time, and arrhythmogenic behavior begin to help us characterize arrhythmia substrate. This methodology can help uncover the mechanisms for the arrhythmia, and part of our future directions is to use this platform to test therapeutics for si-IVF patients. We also plan to study a CRISPR edited version of this same patient line to understand the contribution of a VUS (variant of unknown significance) to arrhythmia substrate. Further, we plan experimentation to include conducting fluorescent optical mapping and CaT analysis on iPS-CMs co-cultured with cardiac fibroblasts on a patterned PDMS substrate to gain mechanistic insights on this case of si-IVF using a more physiologic investigation platform.

Patient-Specific Human Induced Pluripotent Stem Cell-Derived Engineered Cardiac Tissue Model Of Hypertrophic Cardiomyopathy

Jake A. Melby[1,2], Kalina Reese[3], Willem de Lange[4], Jianhua Zhang[5], Gina Kim[5], Timothy J. Kamp[3,5], J. Carter Ralphe[4], and Ying Ge[1,3,6]

[1]Department of Chemistry, University of Wisconsin-Madison
[2]Training Program in Translational Cardiovascular Science, University of Wisconsin-Madison
[3]Department of Cell and Regenerative Biology, University of Wisconsin-Madison
[4]Department of Pediatrics, University of Wisconsin-Madison
[5]Department of Medicine, University of Wisconsin-Madison
[6]Human Proteomics Program, University of Wisconsin-Madison

Background: Hypertrophic cardiomyopathy (HCM) is a commonly heritable cardiovascular disease that results in the thickening of the ventricular septum and is the leading cause of sudden cardiac death in young adults. While around 1,500 mutations contributing to the HCM phenotype have been identified in at least 19 genes encoding sarcomeric proteins, the molecular events leading to the disease phenotype remain largely unknown. Previous studies using a 2-dimensional human induced pluripotent stem cell-derived cardiomyocytes (hiPSC-CM) monolayer model of HCM successfully demonstrated characteristics of the HCM phenotype observed in the adult myocardium including abnormal Ca^{2+} handling, cellular hypertrophy, and arrhythmia [1]; however, hiPSC-CM model systems remain underdeveloped. 3-dimensional engineered cardiac tissue (ECT) constructs made from hiPSC-CMs have emerged as appealing disease model systems due to their closer representation of the structural and functional complexity of the heart. Herein, we have leveraged the power of tissue engineering, functional assessments, and proteomics technologies to study the underlying molecular events leading to HCM pathogenesis.

Methods: hiPSC-ECTs generated from a family with control (no mutation) and HCM (R663H mutation in beta myosin heavy chain) lines were assessed using an integrated method [2] that permits sequential analysis of functional properties and top-down mass spectrometry (MS)-based proteomics. Isometric twitch force measurements were performed to characterize contractile performance between the control and HCM hiPSC-ECTs. Using the exact same hiPSC-ECT constructs, sarcomere proteins were extracted and analyzed using a top-down liquid chromatography (LC)-MS based approach to quantify sarcomere protein isoforms and post-translational modifications. Additionally, global bottom-up proteomics was performed on a separate group of control and HCM hiPSC-ECTs to quantify protein expression differences.

Results: The HCM hiPSC-ECTs displayed a prolonged time for contraction and relaxation kinetics compared to the control hiPSC-ECTs. Furthermore, the twitch force magnitude was lower in the HCM hiPSC-ECTs, although not statistically significant. Several sarcomeric proteoforms from the functionally tested hiPSC-ECTs were analyzed via top-down LC-MS with significant changes in total phosphorylation for sarcomere proteoforms such as α-tropomyosin and cardiac troponin T. Global bottom-up proteomics data determined that proteins related to the extracellular matrix were downregulated and proteins related to cell remodeling and metabolism were upregulated in the HCM samples.

Discussion: Our results revealed that the kinetics, twitch force magnitude, and sarcomere proteoform landscape of the HCM hiPSC-ECTs were altered compared to the control hiPSC-ECTs. For the first time, we were able to correlate between the measured contractile parameters and the PTMs of sarcomeric proteins between the two groups of hiPSC-ECTs. The bottom-up proteomics data found significant changes in several non-sarcomeric proteins, which offers new insights into this disease traditionally coined the "disease of the sarcomere." By integrating innovative tissue engineering techniques, functional assessments, and proteomics technologies, we can uncover the underlying disease progressions for HCM and empower further studies for cardiac disease modeling and drug discovery.

Elucidating The Role Of Mechanistic Target Of Rapapmycin Complex 1 During Heart Regeneration

Wyatt Paltzer[1], Jiyoung Bae[2], Ahmed Mahmoud[2]

[1]Department of Genetics, University of Wisconsin-Madison
[2]Department of Cell and Regenerative Biology, University of Wisconsin-Madison

Background: Heart failure is the leading cause of morbidity and mortality worldwide, with no current therapeutic interventions. Stimulation of adult heart regeneration to replace the damaged cardiac tissue has enormous therapeutic potential for treatment of heart failure. In contrast to the adult heart, the neonatal mouse heart demonstrates a remarkable ability to regenerate after injury, which presents a unique model to study the mechanisms that regulate heart regeneration. During cardiomyocyte maturation a metabolic shift occurs, where the primary energy source shifts from glycolysis to fatty acid oxidation, this metabolic shift results in the loss of heart regeneration. Recent work in our lab showed that promotion of glycolysis after adult myocardial infarction injury can promote heart regeneration. Interestingly, a recent study demonstrated that mechanistic Target of Rapamycin Complex 1 (mTORC1) hyperactivity shifted the primary energy source to glycolysis from fatty acid oxidation in the adult heart. However, the role of mTORC1 in heart regeneration is not yet defined. Thus, we hypothesize that mTORC1 will be required for heart regeneration, and hyperactivation of mTORC1 will stimulate adult heart regeneration. Elucidating the role of mTORC1 during heart regeneration will provide key insights on the metabolic regulation during heart regeneration, as well as uncover potential targets for therapeutic intervention to stimulate adult heart regeneration.

Methods: To examine the role of mTORC1 during heart regeneration I utilized the neonatal mouse myocardial infarction (MI) model. In this model a suture was ligated around the left anterior descending artery, preventing blood flow to the left ventricle. This resulted in a clinically significant MI in the left ventricle that is similar to those observed in human patients. Mice were then treated with the mTORC1 inhibitors rapamycin or everolimus during the regenerative period. Regeneration was then analyzed via histological and immunofluorescent techniques to examine the requirement of mTORC1 during neonatal heart regeneration.

Results: mTORC1 inhibition during neonatal regeneration prevents the endogenous heart regeneration, resulting in cardiac hypertrophy and scar tissue formation. As cardiomyocyte proliferation is key to regeneration through replenishing the damaged myocardium with new cardiomyocytes, we next examined cardiomyocyte proliferation, which demonstrated that mTORC1 inhibition significantly decreases cardiomyocyte proliferation after MI. However, it is not yet clear how mTORC1 inhibition led to the reduction in cardiomyocyte proliferation that resulted in the loss of heart regeneration, thus warranting further studies.

Discussion: Previous literature demonstrates that metabolic state during heart regeneration is key to the promotion or inhibition of heart regeneration. We demonstrated that the function of known metabolic regulator mTORC1 is critical for heart regeneration, with mTORC1 inhibition preventing endogenous heart regeneration. Further examinations are needed to examine the mechanism through which mTORC1 inhibition prevents heart regeneration, and whether mTORC1 hyperactivation can stimulate adult heart regeneration.

Valvular Endothelial Cells Regulate Lipid Infiltration In A Sex-Dependent Manner

V. A. Patil*, K. S. Masters
University of Wisconsin – Madison, Madison WI

Background: Calcific Aortic Valve Disease (CAVD) is the most commonly occurring valve disease [1]. CAVD is a progressive disease wherein the valve leaflets undergo a series of changes causing development of fibrotic thickening and calcification, ultimately leading to valvular stenosis [2]. The pathogenesis of CAVD remains poorly understood, but infiltration of low-density lipoproteins (LDL) is a hallmark of early CAVD and is thought to set the stage for further inflammatory and fibrotic events. The aortic valve is covered by a continuous monolayer of valvular endothelial cells (VECs), which should act as a first line of defence against pathological insults such as smoking and hyperlipidaemia [3]. We hypothesize that risk factors such as smoking and hyperlipidaemia cause dysfunction of the protective VEC monolayer via alterations of its glycocalyx, and that these are critical events in LDL infiltration and subsequent valve inflammation. Moreover, because previous studies have established sexual dimorphism in the manifestation of CAVD [4], we propose that VECs exhibit cellular-scale sex differences that influence these pathological outcomes.

Methods: VECs were harvested from healthy porcine aortic valves (Hoesly's Meats, New Glarus, WI) via digestion with a mild collagenase solution followed by cell sorting using FACS to isolate cells positive for CD-31. VECs were cultured in 12-well transwells at 100,000 cells/well for 72 hours in EGM media, switched to 2% FBS EBM media for 2 days, after which a treatment of 100 ug/ml cigarette smoke extract (CSE) was applied for 24h. To determine the effect of CSE on permeability of LDL through the membrane, VECs were incubated with 100 ug/ml Alexa Fluor 488 labelled LDL (AF-488 LDL) for 3 hours and fluorescence readings taken on top and bottom wells. Similarly, to further understand the VEC protective function in context of the whole valve, organ cultures of aortic valve leaflets were incubated with 2% DMEM media overnight then treated with 100 ug/ml CSE, followed by 100 ug/ml AF-488 LDL for 24h. Controls included untreated leaflets and leaflets treated with AF-488 LDL only. The leaflets were then lysed using liquid nitrogen and 10 mg of the powdered lysate was measured and added to 150 ul RIPA lysis buffer for fluorescence measurement. Statistical analysis was performed using a student's t-test between groups with n=3 for all experiments. Glycocalyx shedding was measured via ELISAs for relevant components (e.g., heparan sulfate, CD44), and caveolin-1 was measured via Western blotting.

Results: The barrier function assay showed that treatment with CSE significantly increased the permeability of the VEC monolayer to LDL. These findings suggest that CSE damages the endothelial barrier and glycocalyx and may involve trans localization of Caveolin-1, which is responsible for transporting LDL across the endothelial barrier. There is also much larger significant difference between the female VECs as compared with the male VECs. Similar findings were achieved using ex vivo leaflet organ cultures. Specifically, more LDL infiltrated leaflets incubated with CSE compared to untreated leaflets or those incubated with just AF-488 LDL.

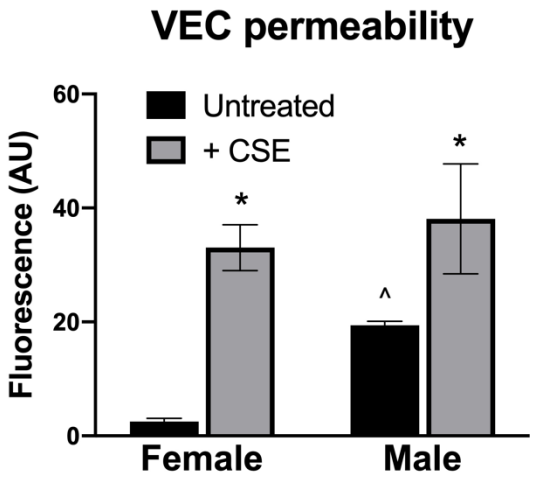

Figure 1: Transwell permeability assay results (N=3) showing the difference between male and female VECs not-treated and treated with 100 ug/ml CSE before incubation with 100 ug/ml AF-488 LDL.

Discussion: These results confirm that CAVD risk factors have an impact on the function of VECs and that there is a sex-related difference involved that may impact how CAVD progresses. Collection of data on glycocalyx shedding and caveolin-1 is ongoing, and future work will examine the inflammatory effects of LDL infiltration.

Poster #17

Top-Down Mass Spectrometry of Phospholamban Proteoforms Enabled By Photocleavable Surfactant

Kalina Reese[a], Jake Melby[b], Kyle Brown[b], Austin Carr[b], Song Jin[b], and Ying Ge[a,b,c*]

[a]*Department of Cellular and Regenerative Biology, University of Wisconsin-Madison*
[b]*Department of Chemistry, University of Wisconsin-Madison*
[c]*Human Proteomics Program, University of Wisconsin-Madison*

Background: Phospholamban (PLN) is a calcium-handling protein in the membrane of the sarcoplasmic reticulum that regulates sarco(endo)plasmic reticulum Ca^{2+}-ATPase 2a (SERCA2a). PLN plays a critical role in the reuptake of calcium ions for muscle contraction, and while not entirely understood, its post-translational modifications (PTMs) dictate its regulatory state. Palmitoylation and phosphorylation of PLN can result in seven different PLN protein products, or proteoforms[1]. Palmitoylation and phosphorylation dysregulation of PLN have been implicated in heart failure (HF); however, there is currently no reliable methodology to accurately identify and quantify PTMs of PLN at site-specific protein residues. Commercially-available antibodies only identify two of the proteoforms with specificity at the phosphoserine16 and phosphorthreonine17 residues. Furthermore, proteomic-based efforts by mass spectrometry (MS) have been unsuccessful due to a lack of MS-compatible surfactants for hydrophobic proteins. Therefore, we have developed a high throughput MS-based top-down proteomics (TDP) protocol that permits identification and quantification of PLN proteoforms from cardiac tissues.

Methods: For our study, we utilized swine cardiac tissues graciously provided the University of Wisconsin-Madison's Cardiac Catheterization Laboratory. Approximately 10 mg of swine tissue was homogenized in ammonium bicarbonate (ABC) cytosolic depletion buffer and centrifuged. Azo[2], an anionic photocleavable surfactant, was then added to the pellet to solubilize the remaining protein pellet. Azo was subsequently cleaved by UV-irradiation. Molecular weight cutoff filters were used to desalt the samples before analysis. The proteins were separated by online reverse-phase liquid chromatography and ionized using electrospray ionization on the Bruker MAXIS II mass spectrometer.

Results: Our novel photocleavable anionic surfactant Azo facilitates reliable extraction of hydrophobic proteins from endogenous swine tissue. Analysis of Azo extracts by TDP reveals various PLN proteoforms across regions of the heart, including single/dual phosphorylation, palmitoylation, and combinations of the like. Furthermore, we localized the palmitoylation to cysteine 36, which is a critical PTM that modulates the interaction of PKA with PLN. Preliminary data also shows potential proteoform differences between the right and left ventricle of a control sample. To further probe regional heterogeneity, we are applying TDP to characterize PLN in right and left ventricles, right and left atria, and septum using both healthy and HF tissue.

Discussion: Our methodology shows the power of TDP in revealing dynamic proteoform states of PLN, a critical calcium-handling protein in the heart. TDP is particularly promising for PLN research, as traditional bottom-up proteomics (BUP) methods fails to gather site-specific information. Furthermore, BUP cannot be used on many small proteins like PLN due to too few trypic residues. With the knowledge of how PLN proteoforms change from the healthy to diseased heart, we can further understand several cardiac pathologies at a molecular level.

Structural O-Glycoform Heterogeneity Analysis Of The SARS-CoV-2 Spike Receptor Binding Domain For Rational Therapeutic Design To Treat COVID-19

David S. Roberts[1], Morgan Mann[2], Jake A. Melby[1], Eli J. Larson[1], Yanlong Zhu[3,4], Allan R. Brasier[2,5], Song Jin[1], and Ying Ge[1,2,3]

[1]Department of Chemistry, University of Wisconsin-Madison
[2]Department of Medicine, School of Medicine and Public Health, University of Wisconsin-Madison
[3]Human Proteomics Program, School of Medicine and Public Health, University of Wisconsin-Madison
[4]Department of Cell and Regenerative Biology, University of Wisconsin-Madison
[5]Institute for Clinical and Translational Research, University of Wisconsin-Madison

Background: The novel 2019 coronavirus disease (COVID-19) has become a global pandemic, resulting in >700K deaths in the US alone. Severe acute respiratory syndrome coronavirus-2 (SARS-CoV-2), the causative pathogen of COVID-19, utilizes an extensively glycosylated spike (S) protein that protrudes from the viral surface to bind receptor angiotensin-converting enzyme 2 (ACE2) for cell entry. ACE2 is native to the heart and recent studies have established cardiovascular diseases (CVDs) as major comorbidities for COVID-19, with ACE2 mechanistically implicated in myocardial involvement with the disease. Moreover, it has been shown that COVID-19 survivors experience heart damage, regardless of the presence of underlying heart disease. There is growing consensus that S/ACE2 post-translational modifications (PTMs; *e.g.* glycosylation) are heavily implicated in altering viral binding/function, making the detailed analysis of their glycans critical to the development of rationally designed therapeutics for effective treatment and for understanding the specific underlying mechanisms related to the various CVDs. Here, we developed a hybrid native and denaturing top-down mass spectrometry (MS) method for the structural analysis of intact O-glycan proteoforms of the S regional binding domain (S-RBD) to reveal new structural insights of the PTM-landscape of diverse O-glycoforms of the S-RBD.
Methods: Native protein samples were prepared by buffer exchanging into 150 mM ammonium acetate solution by washing the sample five times through a 10 kDa Amicon ultra centrifugal filter (MilliporeSigma, Burlington, MA, USA). Denatured protein samples were reduced using 20 mM tris(2-carboxyethyl)phosphine hydrochloride (TCEP) and followed by buffer exchanging into 0.1% formic acid solution. Native protein samples were analyzed by a timsTOF Pro mass spectrometer (Bruker Daltonics, Bremen, Germany) coupled to a Bruker nanoElute LC system. Intact denatured protein samples were analyzed by nanoelectrospray ionization via direct infusion using a TriVersa Nanomate system (Advion BioSciences, Ithaca, NY, USA) coupled to a solariX XR 12-T Fourier Transform Ion Cyclotron Resonance mass spectrometer (FTICR-MS, Bruker Daltonics, Billerica, MA, USA) for denatured analysis. Tandem mass spectra were output from the DataAnalysis 4.3 software and analyzed using MASH Explorer.
Results: Native trapped ion mobility spectrometry (TIMS)-MS analysis revealed two distinct S-RBD native conformers separated in regional mobility between 0.95 and 1.25 $1/K_0$, which correspond to the S-RBD monomer (z = 8+ to 12+) and dimer (z = 14+ to 16+). Collision cross section (CCS) determined for the native S-RBD O-glycoform monomer (Region 1, 10+ charge state, $^{TIMS}CCS_{N2}$ 2227 ± 4 Å^2) was slightly higher (~50 Å^2) than the theoretical value (~2180 Å^2) calculated using the IMPACT method for the nonglycosylated S-RBD from the X-ray crystal structure (PDB: 6M0J). Top-down MS/MS confidently localized the S-RBD O-glycosite to Thr323 and revealed eight intact O-glycoforms. We found that the relative abundance of Core 1 to Core 2 O-glycan structures was roughly 67:27, with the Core 1 GalNAcGal(NeuAc)$_2$ being the most abundant O-glycoform (~65% relative abundance).
Discussion: We developed a new hybrid top-down MS method to reveal and characterize native S-RBD structural heterogeneity. We report the complete structural characterization of eight S-RBD O-glycoforms along with a Core 2-fucosylated glycan structure not previously reported. Moreover, the relative molecular abundances of each of these intact glycoforms can be quantified, providing new insights into the complex landscape of S-RBD O-glycosylation. The accurate determination of the structure and molecular abundance of intact glycoforms provides the technical foundation to understand the functional significance of these distinct S-RBD glycoforms and emerging S-RBD variants, as well as other O-glycoproteins in general.

Using Novel 4D Strain Imaging To Characterize Murine Cardiac Phenotypes

Allison Rodgers, Jasmine Giles, John Carter Ralphe, Richard Moss, Timothy Hacker

Model Organisms Research Core
Cell and Regenerative Biology

Background: Strain imaging is rooted in speckle-tracking algorithms applied to high-frequency ultrasound images. It is a dimensionless parameter that represents deformation of the heart relative to its original shape. 4D strain imaging is a new technology being developed by Visual Sonics allowing strain measurements across the whole heart, in 3-dimensions over a cardiac cycle. Our objective is to compare cardiac function obtained with 4D strain verses traditional echo in a genetically modified mouse model.

Methods: The mice were genetically modified to affect myosin binding protein c from the Cell and Regenerative Biology lab. Using a Visual Sonics Vevo 3100 preclinical imaging system outfitted with the MX400 transducer, ~30-MHz, a transthoracic echocardiogram was performed. To begin, mice were sedated by facemask administration of 1% isoflurane, hair removed with Nair, and maintained on a heated platform. Parasternal long axis images of the left ventricle were collected in b-mode, m-mode and as an EKV, ECG-gated Kilohertz Visualization. The probe was rotated and a b-mode and m-mode were taken on the LV in short axis at the same location as the long axis images. A 4D image was then acquired in short axis using the same probe on the 3D motor. Wall and chamber thicknesses were measured on-line from M-mode images obtained in a parasternal long axis view using the leading edge-to-leading edge convention. All parameters were measured over at least three consecutive cardiac cycles and averaged. 4D strain was measured using the SAX 4D cine tracing the edges of the entire LV, in all planes, over the cardiac cycle. The same person obtained all images and measures.

Results: Overall, acquisition of 4D strain data did not significant hindrance to echo. However, due to the alpha nature of the analysis software, the reading of the 4D images was slow. We plan to compare how strain data from the 4D analysis compares to the data from traditional m-mode and EKV images.

Discussion: The potential for 4D strain to evaluate the deformation in the heart over time and across all dimensions is a valuable resource. This may also prove to be an important tool to examine regional changes in cardiac motion. We believe 4d strain will be valuable to uncover subtle and early changes in cardiac function. However, given its novelty, additional data from other murine models is needed to better understand its value.

Poster #20

Mapping Cardiac Innervation During Development, Disease, And Regeneration

Rebecca Salamon[1], Ahmed Mahmoud[1]

[1] Department of Cell and Regenerative Biology,
University of Wisconsin–Madison, USA

Background: The heart relies on the opposing signals from the sympathetic and parasympathetic nerve branches to guide developmental, homeostatic, and repair functions. These intricate neuronal networks are susceptible to injury and fatal misfiring following an adult myocardial infarction (MI). Remarkably, an MI in the neonatal mouse results in robust regeneration and restoration of autonomic functions. Yet, the patterning of cardiac innervation influencing these states of development, disease, and repair is not well understood. In this work, we are mapping the cardiac innervation patterns that allow for regulation of these essential functions.

Methods: We are analyzing the spatial patterning of cardiac innervation by employing heart clearing, whole-mount staining, and three-dimensional imaging techniques.

Results: We are particularly interested in mapping the parasympathetic nerves, which have often been overlooked as a contributor to ventricular innervation. Excitingly, our preliminary results show dense parasympathetic axon bundles present throughout the ventricles of the heart, a finding that has not been described in previous literature. Moreover, the parasympathetic and sympathetic nerve fibers are intertwined in the ventricles through a developmental patterning mechanism that we look forward to further exploring. Our lab has also discovered that the parasympathetic nerves regulate neonatal heart regeneration. Here, we show preliminary data of reinnervation uniquely occurring during neonatal heart regeneration.

Discussion: The results of our research can expand our knowledge of the development and plasticity of the cardiac nervous system.

Enhanced Mechanical Function Of Cardiomyocytes Using Micropatterning And Co-Culture With Human iPSC-Derived Cardiac Fibroblasts

Alana Stempien[1,2], Brett N. Napiwocki[1,2], Di Lang[3], Rachel Kruepke[4], Gina Kim[3], Jianhua Zhang[3], Lee L. Eckhardt[3], Alexey V. Glukhov[3], Timothy J. Kamp[3,5], Wendy C. Crone[1,2,4,6]

[1]*Department of Biomedical Engineering, University of Wisconsin-Madison*
[2]*Wisconsin Institute for Discovery, University of Wisconsin-Madison*
[3]*Departmetn of Medicine, Division of Cardiovascular Medicine, University of Wisconsin-Madison*
[4]*Engineering Mechanics Program, University of Wisconsin-Madison*
[5]*Department of Cell and Regenerative Biology, University of Wisconsin-Madison*
[6]*Department of Engineering Physics, University of Wisconsin-Madison, Madison, WI, USA*

Background: While cardiomyocytes (CMs) are the cell type primarily responsible for contraction in the heart, cardiac fibroblasts (CFs) also play an important role in maintaining cardiac function including synthesis, remodeling, and degradation of the extracellular matrix (ECM), as well as cell-cell communication with CMs. Thus, in vitro co-culture models that allow for control of myocyte-fibroblast interactions while maintaining the spatial arrangement of the cells could provide a better understanding of the influence of CFs on CM function.

Methods: We used a previously validated 2D micropatterned platform that provides control over ECM geometry while utilizing polydimethylsiloxane (PDMS) with a physiologically relevant substrate stiffness. The lane width influenced CM shape and sarcomere organization by providing defined attachment regions, and the bridges increased connectivity which produces synchronized contractions across large arrays of CMs. Human pluripotent stem cell-derived CFs and CMs were co-cultured using a CM:CF ratio of 10:1. The mechanical properties of CMs were assessed from brightfield videos of synchronized contraction events using digital image correlation (DIC) at days 6, 12 and 18 in culture. Full field second principal strain, which in these experiments represents the contractile strain along the major axis of the CM, was used as the quantitative indicator of functionality (in addition to structural and electrophysiological readouts).

Results: Remodeling and ECM production occurred when CFs were cultured with CMs. After 18 days in culture, the CM-Only condition displayed little collagen and fibronectin, while the co-culture condition showed an abundance of ECM proteins. CFs remodel the ECM into anisotropic fibers when cultured in this platform. Decellularization of these tissues also confirmed a large amount of ECM remodeling and deposition in the co-culture condition compared to the CM-Only condition. DIC measurements demonstrated that at each time point there was increased maximum contractile strain generated in the co-culture condition compared to the CM-Only condition.

Discussion: We have shown that in addition to their influence on ECM, CFs enhance CM function with increased contractile strain in co-culture compared to CMs cultured alone. Our findings highlight the important role CFs play in vivo and the need for co-culture models like the one presented here to provide more representative in vitro cardiac constructs. Future directions involve using CFs to remodel the ECM prior the co-culture of CFs and CMs.

Synthesis of Mannose-6-Phosphonate Conjugate For Targeted Protein Degradation Through The Lysosome

Christopher M. Stevens[1#], Peng Teng[1#], Yaxian Zhou[1#] and Weiping Tang[1]

[1]*Pharmaceutical Sciences Division, University of Wisconsin-Madison School of Pharmacy*
(# These authors contribute equally.)

Background: LYTACs, or Lysosome Targeting Chimeras, are a growing area of targeted protein degradation. These LYTACs are heterobifunctional degraders that can target both a protein of interest and targeting for cell internalization and lysosome degradation. Of the methods available for lysosome targeting, none is more widely applicable than the Mannose-6-phosphate (M6P) and Mannose-6-Phosphate Receptor (M6PR) pathway, however the current LYTACs based on M6P utilize general design and large multivalences of M6P for M6PR binding and cell uptake. Our goal is to create a structurally defined ligand for M6PR binder to streamline LYTAC synthesis and apply it to the degradation of various protein targets of interest.

Methods: Synthesized peptide chains were decorated with a designed Mannose-6-phosphonate. These peptide chains varied in linker distance and composition to study requirements for uptake via the M6PR pathway. The glycoconjugates were linked to a targeting moiety for the protein degradation target (either biotin for initial studies, or an antibody for a specific and relevant target). Several rounds of full chimeras were then tested for uptake in liver cells using a fluorescent based assay, and subsequently quantified for uptake efficacy compared to previous LYTAC models.

Results: Our synthetic route for LYTACs streamlines those previously explored for M6P based lysosome targeting degraders. Initial cell uptake studies have shown effective uptake of target proteins at sub micromolar concentrations of the chimera which validates the refined models. The designed LYTAC proves capable of successfully targeting proteins of interest through both small molecule binders in the model system of biotin and streptavidin and antibodies in the specific degradation of epidermal growth factor receptor (EGFR). Studies to further refine the design and synthesis of the chimera, as well as to expand the potential targets it can degrade, are ongoing.

Discussion: The synthesis of a Mannose-6-phosphonate for conjugation to a peptide backbone has been successful. This synthetic process is streamlined compared to previously explored and is easily conjugated to the peptide backbone through a thiol-ene based reaction. While preliminary cell uptake studies have been successful and the full chimera was able to bring both a model target and a specific relevant target into a cell with good effectivity, there remains further areas for exploration in increasing synthetic efficiency and application to degrading a target of interest. We plan to utilize the most efficacious LYTAC to degrade relevant proteins in cardiovascular diseases and other diseases.

Conformation Sensitive Antibody Reveals An Altered Cytosolic PAS/CNBh Assembly During hERG Channel Gating

Whitney A. Stevens-Sostre[1], Carol A. Harley[2,3], Ganeko Bernardo-Seisdedos[4], David K. Jones[5], Maria M. Azevedo[2,3], Paula Sampiao[2,3], Marta Lorga-Gomes[2,3], Matthew C. Trudeau[6], Oscar Millet[4], Gail A. Robertson[1], Joao H. Morais Cabral[2,3]

[1]Department of Neuroscience, University of Wisconsin-Madison, Madison, WI, USA
[2]Instituto de Investigação e Inovação em Saúde da Universidade do Porto (i3S), Porto, Portugal
[3]Instituto de Biologia Molecular e Celular (IBMC), Universidade do Porto, Porto, Portugal [4]Department of Structural Biology, Protein Stability and Inherited Disease Laboratory, Center for Cooperative Research in Biosciences CIC bioGUNE, Derio, Spain
[5]Department of Pharmacology, Universityof Michigan Medical School, Ann Arbor, MI, USA [6]Department of Physiology, University of Maryland School of Medicine, Baltimore, MD, USA

The human ether-à-go-go-related gene (hERG) K^+ channel has a crucial function in cardiac repolarization and mutations or channel block can give rise to long QT syndrome and catastrophic ventricular arrhythmias. The cytosolic assembly formed by the N-terminal Per-Arnt-Sim (PAS) and C-terminal cyclic nucleotide binding homology (CNBh) domains is the defining structural feature of hERG and related KCNH channels. However, the molecular role of these two domains in channel gating remains unclear. We have previously shown that single-chain fragment variable (scFv) antibody fragments can modulate hERG function by binding to the PAS domain. Here, we mapped the scFv2.12 epitope to the PAS/CNBh domain interface using NMR spectroscopy and site-directed mutagenesis. We show using ELISA competition assays and in-cell Förster resonance energy transfer (FRET) that scFv binding is incompatible with the PAS/CNBh interaction. By generating a fluorescently labelled scFv2.12, we demonstrate that association with the full-length hERG channel is state-dependent. We detect FRET withscFv2.12 when the channel gate is open but not when it is closed. In addition, state dependence of scFv2.12 FRET signal disappears when the R56Q mutation, known to destabilize the PAS/CNBh interaction, is introduced in the channel. Altogether, these data demonstrate the PAS/CNBh assembly is stabilized when the gate closes and destabilized when the cytosolic gate opens, favoring PAS domain dissociation from the CNBh domain. Work was supported by NIH grants F99NS125824 (WASS), 1R01NS081320 (GAR, JHMC) and 1R01HL131403 (GAR), R01 GM130701 (MCT) and Agencia Estatal de Investigación grant RTI2018- 101269-B-I00 (OM).

Native Mass Spectrometry Of Human Cardiac Troponin Complexes Enabled By Functionalized Nanoparticle Enrichment And Online Size Exclusion Chromatography

Timothy N. Tiambeng[1], Jake A. Melby[1], David S. Roberts[1], Kyle A. Brown[1], Emily A. Chapman[1], Timothy J. Aballo[1,2], Daniel Kim[1] , William H. Swain[1], Andrew J. Alpert[1,3], Song Jin[1], Ying Ge[1,2,4]

[1]Department of Chemistry, University of Wisconsin-Madison, Madison, WI 53705
[2]Department of Cell and Regenerative Biology, University of Wisconsin-Madison, Madison, WI, 53705
[3]PolyLC, Columbia, MD, 21045
[4]Human Proteomics Program, School of Medicine and Public Health, University of Wisconsin-Madison, Madison, 53705

Background: The cardiac troponin complex (cTn, ~77 kDa) consists of three subunits (troponin I, T, and C), and plays critical roles in cardiac function. Following a heart attack, cTn is released into circulation mainly as a ternary ITC complex, with cTnI and cTnT recognized as cardiac-specific diagnostic biomarkers. However, methods to characterize intact cTn by native MS remain lacking due to the challenges in the isolation and preservation of cTn under non-denaturing conditions. Herein, we report a "native nanoproteomics" strategy incorporating functionalized nanomaterials for specific enrichment of cTn under physiological pH and native size exclusion chromatography (SEC) for rapid online buffer exchange (OBE), thereby enabling the native MS analysis of cTn from human heart samples for the first time.

Methods: Myofilament proteins were extracted from human heart tissue using a LiCl extraction (pH 7.5). Proteins were incubated with surface functionalized, cTnI-targeting nanoparticles to enrich cTn, and eluted natively. SEC (PolyHYDROXYLETHYL A; 100 x 2.1 mm, 5 µm, 200Å) was performed on a Waters nanoAcquity UPLC system for rapid OBE of the cTn complex into MS-compatible mobile phase (200 mM ammonium acetate), and coupled to a quadrupole time of flight (Q-TOF) mass spectrometer (maXis II, Bruker). Offline native SEC fraction collection was also employed for native cTn analysis by nano-electrospray ionization (Advion Triversa Nanomate) coupled to a 12 T Fourier transform ion cyclotron resonance (FTICR) mass spectrometer (SolariX XR, Bruker). All data were processed and analyzed using Compass DataAnalysis and MASH Explorer.

Results/Discussion: We have developed a novel, native nanoproteomics approach that features peptide-functionalized nanoparticles for specific enrichment of cTn and native SEC for rapid OBE, thereby enabling the native MS analysis of cTn from human heart samples. By using a surfactant-free native elution buffer at physiological pH, we successfully eluted cTn as an intact heterotrimer. Native MS analysis revealed noncovalent metallic cofactor protein binding of the native cTn to Ca^{2+} and Mg^{2+}. With native SEC for rapid OBE utilizing 200 mM ammonium acetate (pH 7.0) as mobile phase, proteins and protein complexes were effectively separated from non-volatile buffer components, thereby enabling detection on the Bruker maXis II Q-TOF. Native SEC-MS revealed subunit monomers, cTn dimers (cTnI-cTnC), and native cTn complex trimers (cTnT-cTnI-cTnC, z = 16+ to 20+) that we further analyzed. With respect to the subunit monomers of cTnC, a calcium-binding protein with three divalent cation binding sites, the total calcium binding (Ca_{Total}) was determined to be 1.60 mol Ca^{2+} per mol cTnC, with the doubly Ca^{2+}-bound cTnC proteoform as the most abundant protein species. Additionally, we putatively identifed cTnC proteoforms where Mg^{2+} was occupied in a divalent cation binding site of cTnC. With respect to cTn dimers (cTnI-cTnC), we detected bisphosphorylated cTnI interacting only with the doubly or triply Ca^{2+}-bound proteoform of cTnC, a finding in agreement with existing literature on the physiological interactions of cTnI with Ca^{2+}-bound cTnC. With respect to cTn trimers (cTnT-cTnI-cTnC), we detected only monophosphorylated cTnT, despite the presence of multiple cTnT proteoforms detected from the same human heart sample by denaturing reverse phase liquid chromatography-MS. Monophosphorylated cTnT interacted with bisphosphorylated cTnI, together with unoccupied, singly, doubly, and triply Ca^{2+}-bound proteoforms of cTnC, with the triply Ca^{2+}-bound state of cTnC being the most abundant protein species of the cTn heterotrimer complex.

Atrial-Like Engineered Cardiac Tissue As A Novel In Vitro Cardiac Model

Daniel Turner, BS[1], Willem J. De Lange, PhD[2], Di Lang, PhD[1], Gina C. Kim, BS[1], Timothy J. Kamp, MD[1], Carter J. Ralphe, MD[2], Alexey V. Glukhov, PhD[1]

[1]Department of Medicine-Cardiovascular Medicine, University of Wisconsin-Madison, School of Medicine and Public Health, Madison, WI.
[2]Department of Pediatrics-Pediatric Cardiology, University of Wisconsin-Madison, School of Medicine and Public Health, Madison, WI

Background: Atrial fibrillation (AF) is the most common cardiac rhythm disorder worldwide and a public health burden due to its impact on the risk of stroke, dementia, and heart failure. Despite, its high and growing prevalence, the mechanisms of AF are still poorly understood. This is further limited by the lack of adequate animal and human atrial tissue models. Combining the established methods for producing atrial-like human-induced pluripotent stem cell derived cardiomyocytes (hiPSC-CM) and engineered cardiac tissue (ECT) constructs, we have successfully generated atrial-like ECT.

Methods: Atrial-like and control hiPSC-CM were produced using a GiWi differentiation protocol supplemented with and without 1 mM retinoic acid (RA, to promote atrial-like differentiation), respectively. ECT was generated using Day 30 hiPSC-CM and hiPSC-cardiac fibroblasts mixed with fibrinogen and thrombin and molded via a FlexCell Tissue Train silicone membrane culture plate. Following polymerization of the fibrin matrix, ECTs were cultured for 30 days and then evaluated for action potentials (AP) via optical mapping, mRNA expression via qPCR, and protein expression via Western Blot for atrial-like phenotypes.

Results: Our results demonstrate that atrial ECTs recapitulate various adult cardiac phenotypes that are unattainable by hiPSC-CM in monolayer (ML) culture. First, RA treated atrial-like CM have accelerated beating rates in both ML (two-fold) and ECT form (three-fold) compared to control ML and ECT. Secondly, atrial ECTs demonstrate atrial-like myosin protein expressions with lower ventricular-like MYL2, and higher atrial-like MYL7 expression. Atrial ECTs also exhibit an atrial-like AP with a significantly decreased APD20/APD80 ratio (0.55 vs 0.30 for control and atrial-like ECT, respectively, $P<0.05$), and significantly increased repolarization fraction (0.2 vs. 0.3 for control and atrial-like ECT, respectively, $P<0.05$). Atrial-like ECT mRNA expressions of myosin proteins showed significant reductions in *MYL2* and *MYH7* (90% and 30%, respectively, $P<0.05$) and a significant two-fold increase of *MYL7 (*$P<0.05$), compared to control ECT. Furthermore, atrial ECTs have significantly reduced ventricular progenitor gene *IRX4* (90%, $P<0.05$*)*, and significantly increased atrial-like *KCNJ3* (100%, $P<0.05$*)*. Both control and atrial-like ECT have increased *Cav3* expression (three-fold and two-fold, respectively, $P<0.05$) relative to their respective ML (Fig. 2D), demonstrating improved maturation.

Discussion: Our findings demonstrate the feasibility of generating atrial-like engineered cardiac constructs that may be used to model atrial cardiac diseases such as AF at a cellular and molecular level. Furthermore, these constructs highlight the importance of cardiac fibroblasts in driving changes in cardiomyocyte maturation and function. Due to their ability to be cultured for many weeks, these atrial ECTs will for the first time allow experiments studying the long-term effects of mechanical stress and inflammation that are known to play a significant role in AF pathogenesis.

Investigation Of Anatomically Heterogeneous Transverse Axial Tubule System In Human Atrial Myocardium

Owen Han, Roman Medvedev, Alexey Glukhov

University of Wisconsin-Madison Department of Medicine

Background: Transverse axial tubule system (TATS) represents sarcolemma membrane invaginations that are critically involved in the excitation-contraction (EC) coupling in cardiac myocytes by bringing L-type Ca^{2+} channels and ryanodine receptors in close proximity to ensure synchronous activation of subcellular Ca^{2+} release and contraction. In pathological conditions, disruption of TATS can lead to abnormal impulse propagation and impaired contraction. Compared to ventricular myocytes which have a regular and organized TATS, atrial membrane organization is less organized and varies significantly between cells. Several different subpopulations of atrial myocytes were observed in rat atrium: cells with dense TATS (like in ventricular myocytes), cells with sparse and irregular TATS, and cells without TATS. However, the anatomical localization and spatial distribution of atrial myocytes with different membrane organization remains unknown.

Objective: Our preliminary data from mouse atria suggested a region-specific distribution of TATS. Regional variations in TATS configuration was also observed in large mammalians such as dogs and pigs by other groups. We hypothesized that a region-specific distribution of TATS in human atrial myocytes exists and this organization underlines a region-specific expression of TATS-associated proteins and cell contraction.

Methods: Using confocal microscopy, TATS was imaged and analyzed in 6 regions of healthy human atrium including: left atrial appendage, left atrial free wall, intercaval region (the region between superior and inferior vena cava and between crista terminalis and interatrial septum), right atrium free wall, right atrium appendage, and crista terminalis. TATS was visualized by staining of paraffin embedded tissue slices with wheat germ agglutinin (WGA) conjugated with Alexa-488. Computerized data analysis was performed using an ImageJ routine. TATS density in the specific locations was correlated with the junctophilin-2 protein expression determined by Western blot.

Results: Our data shows that a significant variance of TATS density does exist between human cardiac myocytes from tissues found in different atrial regions. We performed ANOVA statistical comparison between all the regions and found that intercaval region has the highest density of TATS (11.07±5.35% of cell volume), followed by crista terminalis (8.95±3.22%) and both right and left atrial appendage cardiac myocytes (8.95±4.46% and 8.42±3.53, respectively), then by left and right atrial free wall cardiac myocytes (7.11±2.51 and 6.02±2.64, respectively).

Discussion: We observed significant difference in TATS organization between different regions of the human atria. We plan to link these findings with the differences in Ca^{2+} transients and sarcomere shortening in these regions of human atria. The results of this work will foster our understanding of the human atrial normal physiology and may help us find the mechanisms of atrial impairment in diseases. The investigation of the region-specific distribution of atrial myocytes is important for understanding the occurrence of vulnerable regions in cardiac disorders such as heart failure and atrial fibrillation.

RNA Binding Motif 20 (RBM20) Mutation And Phosphorylation In Cardiac Remodelling And Pathogenesis

Yanghai Zhang[1], Chunyan Wang[1], Yutong Jin[2], Mei Methawasin[3], Camila Urbano Braz[1], Jeffrey Gao-Hu[1], Betty Yang[1], Joshua Strom[3], Timothy Hacker[4], Hasan Khatib[1], Henk Granzier[3] Ying Ge[2,5,6] and Wei Guo[1,]

[1]Department of Animal and Dairy Sciences, University of Wisconsin-Madison, Madison, WI
[2]Department of Chemistry, University of Wisconsin-Madison, Madison, WI
[3]Department of Molecular and Cellular Medicine, University of Arizona, Tucson, AZ
[4]Division of Cardiovascular Medicine, Department of Medicine, University of Wisconsin School of Medicine and Public Health, Madison, WI
[5]Department of Cell and Regenerative Biology, School of Medicine and Public Health, University of Wisconsin-Madison, Madison, WI
[6]Human Proteomics Program, School of Medicine and Public Health, University of Wisconsin-Madison, Madison, WI

Background: Genetic mutations may gain new molecular function and result in diseases. Genetic studies show that mutations in a gene named as RNA binding motif 20 (RBM20) are associated with severe dilated cardiomyopathy (DCM) and death at young age.

Methods: To test whether Rbm20 mutations are responsible for cardiac remodelling and pathogenesis, we selected two mutations (S637A and S639G) located in arginine/serine (RS)-rich domain of RBM20 and generated two knock-in (KI) mouse models (*Rbm20*^{S637A} and *Rbm20*^{S639G}) respectively. Histological and anatomical analysis and echocardiography were conducted to assess morphological and functional changes of the heart in both mouse lines. RNA-seq was performed to analyse the differentially expressed (DEGs) and spliced genes (DSGs). In addition, force measurements and Ca^{2+} transient evaluation of intact myocytes were performed. The immunostaining was carried out to determine nucleocytoplasm transport of RBM20. Middle down mass spectrometry (MS) was performed to identify phosphorylation of RBM20 and *in vitro* cell culture study was used to examine the role of RBM20 phosphorylation in protein trafficking.

Results: Our results revealed that KI male and female mice from both mouse lines displayed enlarged left ventricular chamber, thinner ventricular walls, reduced ejection fraction, and high premature death rate. RNA-seq analysis showed that DEGs and DSGs involved in arrhythmia, cardiomyopathy, and calcium handling in both mouse lines. In addition, the cellular diastolic stiffness was reduced in KI mice. Immunostaining in tissues and single cardiomyocytes respectively showed both mutations promote RBM20 nucleocytoplasmic trafficking and granules formation. Totaling 16 phosphorylation sites were identified with MS including S637 (S638 in rat and S635 in human) and S639 (S640 in rat and S637 in human) in RBM20. *In vitro* study showed that phosphorylation is not a major cause for RBM20 re-localization and granules formation.

Discussion: RBM20 mutations are gain-of-function mutations, leading to heart failure and premature death. The phosphorylation does not play a role in RBM20 trafficking and granules formation, but mutation does reduce the phosphorylation level *in vivo*. However, the role of phosphorylation in heart failure progression remains to be determined.

RyR2 With Three Major Phosphorylation Sites Ablated Shows Blunted Luminal Ca^{2+} Sensitivity And Increased Early After Depolarization Susceptibility

Jingjing Zheng, Holly Dooge, Héctor H. Valdivia, Francisco J. Alvarado

[1]Department of Medicine, Division of Cardiovascular Medicine, and Cardiovascular Research Center, University of Wisconsin-Madison School of Medicine and Public Health, Madison, Wisconsin, USA

Background: Ca^{2+} release through ryanodine receptor 2 (RyR2) is an essential component of cardiac excitation-contraction coupling (ECC), the process that converts action potentials (APs) into mechanical contraction. β-adrenergic signaling is a major regulator of ECC through the phosphorylation of specific targets by protein kinase A (PKA) and Ca^{2+}/calmodulin-dependent kinase II (CaMKII). These kinases also phosphorylate RyR2; however, it is not fully understood how the channel is regulated by phosphorylation. To date, only three phospho-residues have been characterized in RyR2: S2030, S2808 and S2814. We created a mouse model with genetic ablation of these three sites (RyR2-S2030A/S2808A/S2814A or triple phospho-mutant [TPM]), to determine the extent to which phosphorylation is required to regulate RyR2 function.

Methods: TPM mice were created at the UW-Madison Biotechnology Center Genome Editing and Animal Models Facility using CRISPR/Cas9 to introduce the S2030A mutation into an existing RyR2-S2808A/S2814A mouse model. The mouse model was validated using Saner sequencing and western blots with phospho-specific antibodies. Mice of 12 weeks of age were used for experiments, including echocardiography, electrocardiography, and simultaneous action potential/Ca^{2+} transient (AP/CaT) recordings in isolated cardiomyocytes. Ca^{2+} sparks were recorded in permeabilized cardiomyocytes at 50 nM cytosolic free [Ca^{2+}].

Results: TPM mice have normal cardiac structure and function compared to WT mice. Remarkably, TPM mice are more susceptible to develop ventricular arrhythmia following the injection of an arrhythmia cocktail. Permeabilized TPM cardiomyocyte show significant fewer Ca^{2+} sparks (3.53±0.33 vs. 6.25±0.41 events/s/100 μm in WT, $p < 0.0001$, n = 42 in WT and 43 in TPM) and a higher sarcoplasmic reticulum (SR) Ca^{2+} load than WT (5.36±0.29 TPM, 4.54±0.22 WT, $p = 0.03$). This suggests that TPM cardiomyocytes show less total SR Ca^{2+} leak and that TPM channels have lower activity at diastolic [Ca^{2+}] than WT controls. We evaluated the susceptibility of TPM myocytes to spontaneous Ca^{2+} release (SCR) events in response to frequency by simultaneous AP/CaT recording during a 20 s train of stimulation (1-3 Hz) followed by a 20 s rest period. The propensity to develop SCR was not significantly different between genotypes. Following 3 Hz stimulation, the latency time of the first SCR event is significantly prolonged in TPM myocytes compared to control (11.03±1.66 s vs. 6.27±1.15 s, $p = 0.02$, n = 16 in WT and 14 in TPM). Analysis of AP properties during the stimulation period showed that TPM myocytes are susceptible to develop early depolarizations (EADs). We analyzed only myocytes without any EAD at 1 Hz and found that 31.3% (5 in 16) TPM developed EADs at 2 Hz (compared to none in the WT), while 65% (9 in 14) TPM developed EADs at 3 Hz (compared to only 10% [1 in 10] in the WT). The stimulation frequency also produces a prolongation of the action potential duration at 90% of repolarization (APD90). Compared to APD90 at 1 Hz for each group, TPM cells showed significant prolongation at 3 Hz (125.6±28.6% TPM, 47.2±18.6% WT, $p = 0.03$, n = 15 in TPM and 9 in WT).

Discussion: The data included showing lower Ca^{2+} sparks frequency and higher SR Ca^{2+} load permeabilized cardiomyocytes suggest impaired regulation of TPM channels. The increased propensity to develop ventricular arrhythmia in TPM mice is not explained by diastolic Ca^{2+} release, since we did not observe differences in SCR frequency and latency was prolonged in the TPM. The higher incidence of EADs may contribute to the arrhythmia phenotype we observed in TPM mice under arrhythmia challenge. Additional experiments will be required to explore this mechanism in detail.

Poster #29

Carnitine Palmitoyltransferase (CPT) 1 Promotes Mammalian Heart Regeneration

Jiyoung Bae[1] and Ahmed I. Mahmoud[1]

[1]Department of Cell and Regenerative Biology, University of Wisconsin School of Medicine and Public Health, Madison, WI 53705

Background: A major event in cardiomyocyte maturation that occurs during the transition from a neonatal to an adult state is a metabolic switch in energy utilization by cardiomyocytes. Embryonic and neonatal cardiomyocytes generate energy through glycolysis, while adult cardiomyocytes generate energy through oxidative phosphorylation. Carnitine palmitoyltransferase (CPT)1 is a key enzyme in regulating fatty acid oxidation. CPT1 expression is significantly increased in 7-day-old juvenile mice, which is the time point when mammalian cardiomyocytes exit the cell cycle. Thus, CPT1 could be a key regulator of cardiomyocyte proliferation. However, the role of impaired fatty acid oxidation by CPT1 inhibition during heart failure and regeneration in mouse models remains unclear.

Methods: Here, we investigated the role of etomoxir, CPT1 inhibitor, in regulating postnatal cardiomyocyte proliferation and heart regeneration. Neonatal mice at postnatal day 7 (P7) were used for myocardial infarction (MI) surgery. We performed various analyses, including immunohistochemistry and trichrome staining.

Results: Our results demonstrate that inhibition of CPT1 by etomoxir injection after birth extends the window of cardiomyocyte proliferation in juvenile mice. Remarkably, etomoxir injection to the neonatal mouse heart before and after myocardial infarction injury promotes heart regeneration.

Discussion: CPT1 inhibition by etomoxir promotes postnatal cardiomyocyte proliferation and heart regeneration. These findings support a potentially important new therapeutic approach for human heart failure.

Poster #30

Proteomic Analysis Of Functional Inward Rectifier Potassium Channel (Kir) 2.1 Reveals Several Novel Phosphorylation Sites

Kyle A. Brown[1,2], Corey Anderson[3], Louise Reilly[3], Kunal Sondhi[3], Ying Ge[4,5], Lee L. Eckhardt[3]

Department of Surgery[1]; Department of Chemistry[2]; Cellular and Molecular Arrhythmia Research Program, Division of Cardiovascular Medicine, Department of Medicine[3]; Department of Cell and Regenerative Biology[4], Human Proteomics Program[5], University of Wisconsin-Madison, WI, 53706, USA.

Background: The inward rectifier potassium channel (Kir) 2.1 is crucial for the maintenance of the resting membrane potential and phase-3 repolarization of the cardiac action potential. Several sudden arrhythmic death syndromes including Andersen-Tawil and Short QT syndrome are associated with loss or gain of function mutations in Kir2.1 that are often triggered by changes in β-adrenergic tone. Thus, understanding the posttranslational modifications (PTMs) of this channel (particularly β-adrenergic driven phosphorylation) is important for arrhythmia prevention. Here, we employ proteomic analysis, top-down, middle-down, and bottom-up approaches, for comprehensive characterization of the PTMs of recombinant Kir2.1, resulting in the successful mapping of six novel sites of phosphorylation. In parallel, we utilized whole-cell patch-clamp analysis to verify the function of the channel.

Methods: Kir2.1^{WT} and Kir2.1^{S425A} were stably expressed in HEK293T cells. To confirm that the function of the channel was unaltered by the MYC tag, we performed whole-cell patch-clamp analysis on cells expressing Kir2.1 with and without the tag. Average current-voltage (I-V) data was generated from pcDNA3.1-Kir2.1^{WT} and MYC-Kir2.1^{WT}. For proteomics, the channel was purified by FLAG affinity purification. The purified channel was analyzed by reversed-phase liquid chromatography (RPLC) coupled with mass spectrometry (MS) to acquire an intact protein mass and fragmented (MS/MS) to yielded sequence information including the location of phosphorylation sites. Alternatively, the protein was digested using trypsin or Asp-N and analyzed by RPLC-MS/MS for further phosphorylation site identification.

Results & Discussion: Membrane proteins represent an analytical challenge for proteomic analysis as they are generally expressed at lower levels are hydrophobic, and Kir2.1 specifically is relatively large (~49.5 kDa) in the context of top-down proteomics. Here, we utilized MYC-tag affinity purification to enrich Kir2.1 from cell lysate generated using a nonionic surfactant, DDM, and found that a low pH elution condition (1% formic acid) lead to the highest recovery. RPLC was successfully utilized to separate Kir2.1^{WT} from a few co-purified proteins as well as the large residue DDM, resulting in an observed mass of 49,515.7 Da, which is 0.1 Da (2 ppm) lower than the mass corresponding to the amino acid sequence with acetylation (42.0 Da) modification. Top-down analysis enabled the localization of the acetylation to the N-terminus of the protein. Next, the cells expressing the channel were incubated in a PKA stimulating "cocktail" to increase phosphorylation followed by the enrichment and MS analysis. We observed both mono- and bis-phosphorylated Kir2.1^{WT} and successfully localized a phosphorylation site to S425. Based on the identification of S425 phosphorylation, we mutated the site to A to prevent phosphorylation. Interestingly, mon and bis-phosphorylated species were still observed with little change in the overall levels of phosphorylation after mutating S425. Top-down analysis Kir2.1^{S425} enabled the identification of phosphorylation sites at S13 and S14. Finally, we performed bottom-up and middle-down proteomics, which yielded 85% sequence coverage and enabled the identification of additional phosphorylation sites at S313, Y326, and T347 for a total of six phosphorylation site identifications. Kir2.1^{WT} and Kir2.1^{S425A} both displayed a typical inward rectifier N-shape current-voltage relationship using whole-cell patch-clamp analysis. Together the proteomics and functional studies suggest that the overall level of phosphorylation may influence function rather than the specific site; however, further functional analysis is needed to access this trend.

A Hydrophobic Nexus At The Pas-Cap/Globular Pas/CNBHD Interface Tunes Deactivation Kinetics of Herg Channels

Lisandra Flores-Aldama[1], Whitney A. Stevens-Sostre[1], Daniel Bustos Guajardo[2], Gail A. Robertson[1].

[1] Department of Neuroscience, UW-Madison, Madison, WI, USA,
[2]Centro de Investigación de Estudios Avanzados del Maule, Vicerrectoría de Investigación y Postgrado, Universidad Católica del Maule, Talca, Chile.

Slow deactivation is a critical biophysical property of human ether-à-go-go related gene (hERG) channels, mediating the cardiac current IKr during repolarization of the ventricular action potential. Disruption of interactions between the intracellular N-terminal Per-Arnt-Sim (PAS) and C-terminal cyclic nucleotide-binding homology (CNBh) domains can impair slow deactivation and is associated with long QT syndrome (LQTS). The PAS-cap (residues 1-25), an essential mediator of slow deactivation, is composed of an unstructured segment (residues 1-12) and an amphipathic α-helix (residues 13-25). The hERG1a cryo-EM structure positions the PAS-cap α-helix at the interface between the globular PAS (residues 26-135) and CNBh domains, while the unstructured segment is in close contact with the transmembrane domain where it presumably acts to slow deactivation. We analyzed the hERG1a structure and uncovered a hydrophobic nexus between the PAS-cap α-helix and the interface of the globular PAS and CNBh domains. To test the hypothesis that this hydrophobic nexus has an active role in modulating hERG1a deactivation kinetics, we perturbed the hydrophobicity of the region by mutating native residues to serine. Electrophysiology uncovered residues critical for slow deactivation within this hydrophobic nexus. Molecular dynamics simulations showed that serine substitutions did not disrupt the conformation of the PAS-cap helix, and instead caused a rearrangement of the hydrophobic interactions between the PAS-cap α-helix and neighboring residues at the globular PAS and CNBh domains. These results suggest that hydrophobicity at this nexus positions the PAS-cap α-helix, promoting engagement of the upstream unstructured segment mediating slow deactivation. Interestingly, several LQTS disease mutations lie at this interface, underscoring the importance of this novel role for the PAS-cap α-helix in hERG gating. Supported by NINDS F99NS125824 (WASS) and 1R01NS081320 (GAR)

Poster #32

Towards A Better Understanding Of The Function And Regulation Of LRRC10 In The Heart

Zachery R. Gregorich[1], Youngsook Lee[2], Timothy J. Kamp[1,2]

[1]Department of Medicine
[2]Department of Cell and Regenerative Biology

Background: Leucine-rich repeat containing protein 10 (LRRC10) is a member of the Leucine-rich repeat containing (LRRC) protein superfamily that is expressed almost exclusively in cardiomyocytes. LRRC10 is expressed in the developing heart, upregulated at birth, and a high level of expression is maintained throughout adulthood. Interestingly, prior studies have linked LRRC10 variants to dilated cardiomyopathy and, more recently, LRRC10 has been implicated in cardiac regeneration. Despite the cardiac-specific expression pattern and mounting evidence indicating a critical role for LRRC10 in cardiac function, little remains known about this protein. Towards a better understanding of the function and regulation of LRRC10 in the heart, herein, we sought to identify putative LRRC10-interacting proteins and phosphorylation sites.

Methods: GST-tagged LRRC10 was expressed in bacteria, purified using Glutathione-Agarose (Sigma), and incubated with mouse heart lysate. Bound proteins were digested on-bead to peptides and identified using bottom-up mass spectrometry (MS). EGFP-tagged ARHGEF17 and MYC/6xHis-tagged LRRC10 were co-expressed in HEK293 cells and co-immunoprecipitated (co-IP) using anti-LRRC10 (YenZym) and anti-ARHGEF17 (Abcam) antibodies. Recovery of LRRC10 and ARHGEF17 in the co-IPs was assessed by Western blot with anti-EGFP (Abcam) and anti-MYC (Cell Signaling Technologies) antibodies. Bacterially-expressed GST-tagged LRRC10 and GST alone were phosphorylated *in vitro* with protein kinase A (PKA; New England Biolabs). Phosphorylation of the recombinant proteins was assessed by SDS-PAGE with ProQ Diamond and SYRO Ruby protein gel stains (Thermo Fisher Scientific). Bacterially-expressed 6xHis-tagged LRRC10 was purified by IP using an anti-LRRC10 antibody (YenZym) for top-down MS analysis.

Results: Nineteen putative LRRC10-interacting proteins were identified by bottom-up MS and one of these proteins, ARHGEF17, was selected for further analysis. Co-IP experiments from LRRC10 and ARHGEF17 co-expressing HEK293 cell lysates provided additional support for an interaction between these proteins. Bioinformatics analysis of LRRC10 identified several potential phosphorylation sites within the protein and *in vitro* kinase assays confirmed PKA-mediated phosphorylation of GST-LRRC10, although GST alone was also phosphorylated. IP of 6xHis-tagged LRRC10 expressed in bacteria yielded highly pure protein for top-down MS identification of phosphorylation sites within the protein.

Discussion: Of the potential LRRC10-interacting proteins identified by bottom-up MS in our initial screen, ARHGEF17 was selected for further analysis based on evidence in the literature implicating the protein in the control of cell division—an interaction that could play a part in the LRRC10-mediated regenerative response. The results of our co-IP experiments in HEK293 cells support an interaction between LRRC10 and ARHGEF17; yet, demonstration of this interaction in the heart is still under investigation and will be a necessary next step to confirm this interaction. Bioinformatics analysis and the results of our *in vitro* kinase assays suggest that LRRC10 may be regulated by phosphorylation, although identification of the specific phosphorylation sites and evidence for endogenous phosphorylation of the protein in the heart remain to be established.

Grayscale Ultrasound Texture Features Of Carotid And Brachial Arteries In People With HIV Infection Before And After Antiretroviral Therapy

*[1]Christina M Hughey, MD; *[1]Belinda M. Vuong, MD; [2]Heather B. Ribaudo, PhD; [1]Carol C. K. Mitchell, PhD; [1]Claudia E. Korcarz, DVM;
[3]Howard N. Hodis, MD, [4]Judith S. Currier, MD, MSc; [1]James H. Stein, MD *co-first authors

[1]University of Wisconsin School of Medicine and Public Health; Madison, WI [2]Harvard T.H. Chan School of Public Health; Boston, MA [3] Keck School of Medicine of USC, Los Angeles, CA [4]David Geffen School of Medicine at University of California-Los Angeles; Los Angeles, CA

Background: To investigate relationships between atherosclerotic cardiovascular disease (ASCVD) risk factors, markers of human immunodeficiency virus (HIV) infection, inflammation, and the effect of antiretroviral therapy (ART) on the arterial wall.

Methods: A5260s was a prospective, 144-week study of ART-naive people with HIV infection who were randomized to three ART regimens. We performed grayscale ultrasound image analyses of the common carotid and brachial arteries prior to and after successful ART (i) to measure arterial wall echogenicity using the grayscale median pixel intensity (GSM) and (ii) to extract texture features of contrast (using the gray-level difference statistic method, GLDS-CON) and entropy.

Results: Among 201 ART-treated and suppressed participants, carotid artery GSM correlated strongly with several ASCVD risk factors before and after ART, but not markers of HIV infection. Changes in all 3 gray scale measures from baseline to 144 weeks correlated consistently with changes in sCD163: GSM (p=0.044), GLDS-CON (p=0.024), and entropy (p=0.016). Atazanavir/ritonavir-containing ART was associated with an increase in entropy (p=0.05), but not GSM or GLDS-CON. Correlations of brachial artery grayscale measures were weaker.

Discussion: In ART-naïve people living with HIV infection, carotid artery grayscale ultrasound measures are associated with traditional ASCVD risk factors, not markers of HIV disease severity or inflammatory biomarkers. Reductions in sCD163 following ART initiation were associated with consistent improvements in all three carotid artery grayscale measures, suggesting that reductions in macrophage activation with ART initiation may lead to less arterial injury and reduce ASCVD risk.

RNA Binding Proteins Associated With Translation Of hERG1a And 1b In The Heart

Jennifer J. Knickelbine[1,2], Yusi Cui[3], Fang Liu[1], Daniela Beltran Hernandez[1], Jin Li[1], Catherine A. Eichel[1], Lingjun Li[3,4], Gail A. Robertson[1,2]

[1]*Department of Neuroscience, University of Wisconsin-Madison*
[2]*Training Program in Translational Cardiovascular Science, University of Wisconsin-Madison*
[3]*Department of Chemistry, University of Wisconsin-Madison*
[4]*School of Pharmacy, University of Wisconsin-Madison*

Background: The expression of cardiac ion channels must be precisely controlled to produce the regular beating of the heart and protect from arrhythmia. Many studies have documented the functional properties of these channels, key amino acid residues, and post-translational modifications, but much less is known about how the subunits of a given ion channel assemble or how their mRNA transcripts are regulated. My project aims to determine the mechanism of co-translational association between two related subunits (1a and 1b) of the hERG voltage-gated potassium channel, which is responsible for the major repolarizing current in the cardiac action potential. The magnitude and gating of the tetrameric channel are greatly affected by subunit composition, with heteromeric channels conducting much more current than either homomeric channel. This makes appropriate assembly of the channel subunits vital, as impaired conductance can prolong the cardiac action potential and cause long QT syndrome and sudden cardiac death.

Methods: Previous work in the lab has shown that hERG 1a and 1b mRNAs co-purify with nascent hERG 1a protein from lysates of co-transfected HEK 293T cells, cardiomyocytes derived from induced pluripotent stem cells (iPSC-CMs), and native myocardium. This association is not dependent on synthesis of nascent 1b protein, and knockdown of either transcript reduces the levels of both transcripts, suggesting that the association likely occurs at the mRNA level. This project used affinity purification mass spectrometry (AP-MS) to identify RNA binding proteins (RBPs) that associate with the 1a and 1b transcripts in HEK 293T cells. We used gene ontology, Genome Wide Association Studies (GWAS), and known roles in mRNA localization/trafficking and translation initiation to narrow the list to 11 candidates for further study. We are further validating hERG-RBP interactions in iPSC-CMs and heart tissue using co-IP, colocalization by single molecule fluorescence *in situ* hybridization (smFISH) and immunofluorescence (IF), proximity ligation assays (PLAs), and shRNA knockdown of candidate interacting RBPs.

Results and Discussion: Our AP-MS analysis yielded 133 proteins that specifically co-purified with hERG using hERG 1a or FLAG antibodies, 55 of which have RNA binding gene ontology, and included RNA helicases, splicing factors, nuclear pore subunits, and chaperones/ER quality control machinery. We selected 11 of these for further study based on their reported function in mRNA localization/trafficking and translation initiation, GWAS ties to hERG-related functions in the heart and brain, and availability of suitably specific antibodies. Preliminary validation of four of these RBPs (DDX3, DDX5, GCN1L1, TBL2) confirms association by co-immunoprecipitation with RBP-specific antibodies and co-localization in iPSC-CMs using single molecule fluorescence *in situ* hybridization (smFISH) and immunofluorescence. Ongoing experiments aim to confirm association within 40 nm using proximity ligation assays (PLAs) and determine the effect of shRNA knockdown of these RBPs on hERG complex formation and function.

Region-Specific Distribution Of Transversal-Axial Tubule System Organization Underlies Heterogeneity Of Calcium Dynamics In The Atrium

Xiaoyu Yuan, Roman Y. Medvedev, Lucas Ratajczyk, Owen Y. Han, Di Lang*, Alexey V. Glukhov*

Department of Medicine, University of Wisconsin-Madison School of Medicine and Public Health, Madison, Wisconsin 53705, USA

Background: T-tubules are sarcolemmal membrane invaginations which play an integral role in synchronizing Ca^{2+} releases and triggering contraction in cardiomyocytes. Unlike in ventricles, atrial myocytes have a more complex transverse-axial tubule system (TATS) which is heterogeneously expressed throughout the atria, while the exact anatomical distribution and its impact on Ca^{2+} dynamics remains unknown.

Methods: *Ex vivo* live mouse atrial preparations were mounted onto custom-made setup and imaged using Leica SP5 confocal microscope under high magnification objectives (63×, N.A. 1.40 and 40×, N.A. 1.30). Mosaic scanning patten was applied to image the whole atrial preparation. A novel Matlab-based computational algorithm was developed for automated analysis of TATS integrity from the stack of images acquired. Ca^{2+} dynamics was optically mapped from isolated atrial preparations using high-speed and high-resolution cameras, and imaged in isolated atrial myocytes using scanning confocal microscope. Detubulation was applied in isolated atrial myocytes to identify the role of TATS in the synchronization of subcellular Ca^{2+} releases.

Results: We have unveiled a region-specific distribution of TATS in the mouse right atrium where tubulated myocytes were predominantly localized within the right atria appendage (RAA) and partially tubulated/untubulated myocytes were located within the intercaval region (ICR): 0.72 ± 0.01 a.u. for RAA versus 0.66 ± 0.02 a.u. for ICR, $P<0.05$. This region-specific TATS distribution was correlated with heterogeneous Ca^{2+} dynamics throughout mouse right atrium. Specifically, the subcellular Ca^{2+} releases were less synchronized in the partially tubulated/untubulated atrial myocytes which is characterized by the prolonged Ca^{2+} transient rise-up time observed in both whole atrial preparation ICR region (6.84 ± 0.45 ms in RAA versus 9.14 ± 0.47 ms in ICR, $P<0.05$) and isolated ICR myocytes (18.24 ± 2.18 ms in RAA cells versus 28.18 ± 3.13 ms in ICR cells, $P<0.05$). Importantly, these difference in the subcellular Ca^{2+} release synchronization was abolished by the detubulation in the myocytes isolated from RAA region confirming a crucial role of TATS in Ca^{2+} transient synchronization.

Discussion: Our findings indicate a different role of TATS in Ca^{2+} signaling at distinct anatomical regions of the atria and could potentially provide mechanistic insight into pathological atrial remodeling associated with changes in TATS organization.

Stretch-Induced Caveolae-Mediated Disruption Of cAMP Microdomains Leads To Arrhythmogenic Ca^{2+} Mishandling In Mouse Atrial Myocytes

Roman Y. Medvedev, Frank C. DeGuire, Alexey V. Glukhov

Department of Medicine, Cardiovascular Medicine,
University of Wisconsin-Madison School of Medicine and Public Health,
Madison, Wisconsin 53705, USA

Background: Atrial fibrillation (AF) often occurs in the settings of atrial pressure/volume overload and is associated with pathologically elevated cardiomyocyte stretch. Mechanism of ectopic beats, that trigger AF, has been linked to Ca^{2+} mishandling and leaky ryanodine receptors (RyRs), while the cause of RyRs dysfunction remains elusive. Caveolae membrane structures are involved in both mechanosensing and mechano-chemical feedback via modulation of cAMP signaling. Here, we hypothesize that stretch disrupts caveolae, stimulating cAMP production and leading to sarcoplasmic reticulum (SR) Ca^{2+} leak via augmentation of RyRs phosphorylation.

Methods and Results: Cell size analysis and Ca^{2+} dynamics measurements were performed by confocal imaging of isolated wild type (WT) mouse atrial myocytes. Cell stretch was modeled by hypoosmotic swelling (from 310 mOsM to 210 mOsM) and resulted in ~30% increase in cell width ($p<0.05$) with no change in cell length. Swelling resulted in a biphasic effect on Ca^{2+} spark activity: a fast (<10 min of exposure) ~50% increase ($p<0.001$) followed by a slow decrease to the level observed in isotonic conditions (>30 min of exposure). Spontaneous Ca^{2+} release activity was significantly exacerbated under β-adrenergic stimulation (100 nM isoproterenol): a number of Ca^{2+} waves increased from 22% in control cells to 62% in swelled cells ($p<0.05$). In swelled cells immunofluorescence staining of RyRs, phosphorylated at both protein kinase A (PKA) and Ca^{2+}/calmodulin-dependent protein kinase II (CaMKII) site Ser2808-RyR, showed significant increase as compared to control cells ($p<0.05$). Similarly to swelling, caveolae disruption via cholesterol depletion by 10 mM methyl-β-cyclodextrin (MβCD) or genetic knockout of caveolin-3 led to 2- and 1.5-fold increase in Ca^{2+} sparks frequency, respectively ($p<0.001$). Swelling- and MβCD-induced increases in atrial Ca^{2+} spark activity were prevented via inhibition of (1) cAMP production by adenylyl cyclases by 100 μM SQ22536, (2) PKA by 1 μM H-89, or (3) CaMKII by 1μM KN93. Additionally, stabilization of RyRs by 1 μM dantrolene had no effect of Ca^{2+} sparks in control cells but prevented the swelling-induced increase in SR Ca^{2+} leak. Finally, mouse atrial myocytes from 4-weeks transaortic constriction model of atrial pressure overload showed a 1.6-times higher Ca^{2+} sparks frequency than WT cells ($p<0.01$), which was significantly reduced ($p<0.01$) to WT level after incubation with SQ22536.

Conclusions: Our findings demonstrate that stretch increases spontaneous Ca^{2+} spark activity in mouse atrial myocytes through the disruption of caveolae and associated cAMP-mediated augmentation of PKA and/or CaMKII activity. This mechanism could be involved in Ca^{2+}mishandling and AF development in pressure overloaded hearts.

Poster #37

Novel Role Of Compound 21, An Angiotensin Type 2 Receptor Agonist In Inducing Angiogenesis In Pregnant Human Uterine Artery Endothelial Cells

Jay Mishra[1], Sri Dangudubiyyam[1], Ruolin Song[1], Sathish Kumar[1, 2]

[1]Department of Comparative Biosciences, School of Veterinary Medicine, University of Wisconsin, Madison, WI 53706, USA.
[2]Department of Obstetrics and Gynecology, School of Medicine and Public Health, University of Wisconsin, Madison, WI 53792, USA.

Background: Angiogenesis is vital for placental vascular development and uterine artery remodeling, leading to a low-resistance and a low-pressure system in pregnancy. The Renin-angiotensin system (RAS) is upregulated in pregnancy with increased expression of angiotensin type 2 receptors (AT_2R) and unchanged angiotensin type 1 receptors (AT_1R) in uterine arteries (UA). AT_2R blockade increased vasoconstriction and blood pressure and decreased UA blood flow, indicating that AT_2R plays an important role in modulating vascular function during pregnancy. However, the role of AT_2R in angiogenesis during pregnancy has never been studied. In the present study, using an in vitro model of pregnant human uterine artery endothelial cells (hUAECs) and a selective AT_2R agonist Compound 21 (C21), we evaluated the regulatory effect of AT_2R on angiogenesis and further dissected the mechanistic pathways at transcriptional and translational levels.

Methods: Primary hUAECs established from fresh uterine artery tissues collected from pregnant women (n = 5) undergoing hysterectomy were validated, characterized, and studied at passages 4 to 5. hUAECs were cultured in complete ECM with 5% fetal calf serum and 1% antibiotics and treated with AT2R agonist C21 at 1, 10, and 100 nM doses for 24 hours. Cell proliferation was measured using the MTS cell proliferation assay (Biovision Inc.). Chemotactic motility was assessed using a transwell migration assay in a 24-well Multiwell BD Falcon FluoroBlok Insert System (BD Biosciences). Capillary tube formation was determined in a growth factor–reduced matrigel system. To explore C21 regulated angiogenic pathways, membrane-based angiogenic protein and phosphorylation array (RayBio™ Cytokine Antibody Arrays, RayBiotech) were done. mRNA levels of the target genes were analyzed by qRT-PCR.

Results: AT_2R activation with C21 induced dose-dependent proliferation of hUAECs at 10 and 100 nM doses while 1 nM dose showed a similar effect as vehicle control. Compared to controls, C21 also dose-dependently induced chemotactic motility of hUAECs as determined by transwell migration assay. On matrigel matrix, C21 induced robust capillary-like tube formation. The semiquantitative angiogenesis antibody array showed that C21 induced increased expression of 12 of the 43 angiogenic factors, including EGF, bFGF, Leptin, PLGF, IGF-1, and Angiopoietins. qRT-PCR showed that C21 induced upregulation of these pro-angiogenic proteins at the mRNA level. Surprisingly, C21 did not significantly alter the phosphorylation of proteins related to MAPK, AKT, NFkB, and TGFb pathways.

Discussion: These results, for the first time, show that AT_2R activation significantly increases proliferation, migration, and tube formation in *in vitro* treated hUAECs and that these effects are related to activation of pro-angiogenic proteins such as EGF, bFGF, Leptin, PLGF, IGF-1, and Angiopoietins. The proportional increase in mRNA transcripts suggests that C21 regulates these targets at the transcriptional level. These results identify C21 as a novel agent with therapeutic potential in pregnancy disorders associated with reduced angiogenesis, such as preeclampsia and fetal growth restriction.

Poster #38

Carotid Artery Stiffness Mechanisms Associated With Cardiovascular Disease Events And Incident Hypertension: The Multi-Ethnic Study Of Atherosclerosis (MESA)

Ryan Pewowaruk[1], Claudia Korcarz[1], Yacob Tedla[2], Gregory Burke[3], Philip Greenland[4], Colin Wu[5], Adam Gepner[1]

[1] *University of Wisconsin School of Medicine and Public Health*
[2] *Vanderbilt University School of Medicine*
[3] *Wake Forest School of Medicine*
[4] *Northwestern University Feinberg School of Medicine*
[5] *National Heart, Lung, and Blood Institute*

Background: Elastic arteries stiffen via two main mechanisms: 1) load-dependent stiffening from higher blood pressure (BP), and 2) structural stiffening due to changes in the vessel wall. It is unknown how these mechanisms contribute to incident hypertension and cardiovascular disease (CVD) events.
Methods: The Multi-Ethnic Study of Atherosclerosis (MESA) is a longitudinal study of 6,814 men and women from 6 communities in the United States. MESA participants with B-mode carotid ultrasound and brachial BP at baseline Exam in (2000-2002) and CVD surveillance (mean follow up 14.3 years through 2018) were included (n=5873). Peterson's elastic modulus (PEM) was calculated to represent total arterial stiffness. Structural stiffness was calculated by adjusting PEM to a standard BP of 120/80 mmHg with participant-specific models. Acute load dependent stiffness was the difference between total and structural stiffness. Cox survival models were adjusted for demographics and traditional risk factors,
Results: Load-dependent carotid artery stiffness was significantly associated with higher incidence of CVD events (hazard ratio per 100mmHg [HR] 1.20, 95% CI [1.09 – 1.33], p<0.001) events while higher structural carotid artery stiffness was not (HR 1.03 [0.99 – 1.07], p=0.11). Analysis of participants who were normotensive (BP < 130/80 and no use of antihypertensives) at baseline (n=2122) found higher load-dependent carotid artery stiffness was also associated with significantly higher incidence of hypertension (HR 1.54 [1.35 – 1.75], p<0.001) while higher structural carotid artery stiffness was not (HR 1.03 [0.99 – 1.07], p=0.13).
Discussion: Higher load dependent carotid artery stiffness was significantly associated with future CVD events and incident hypertension, while structural stiffening due to changes in the arterial wall was not. These results provide valuable new insights into the mechanisms underlying the association between arterial stiffness and CVD events. Evaluating the underlying etiology of arterial stiffness could improve CVD risk stratification. Further studies are needed to determine if the underlying mechanisms of arterial stiffness could help further personalize antihypertensive care.

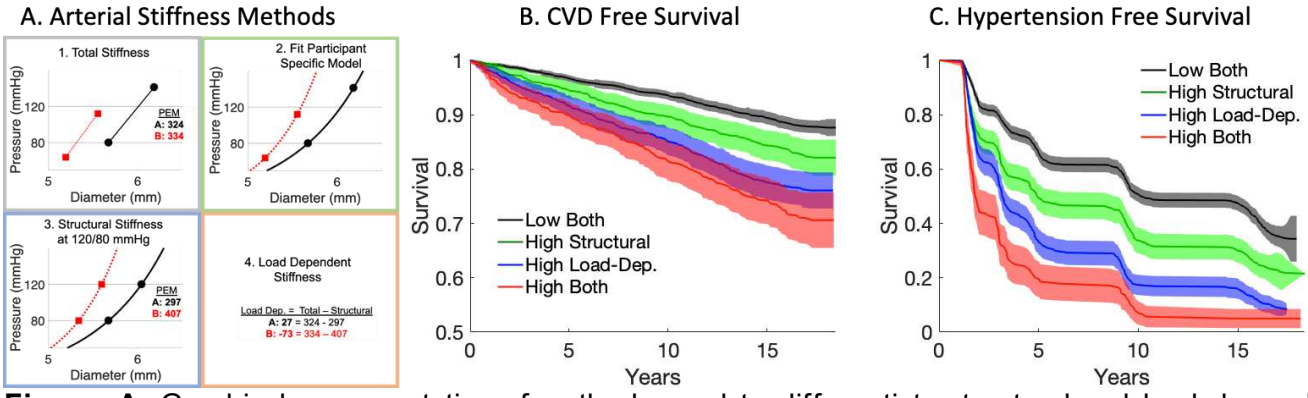

Figure: **A.** Graphical representation of methods used to differentiate structural and load-dependent stiffness. Participants can have similar total stiffness, but via different mechanisms. Kaplan-Meier curves show that **B.** CVD free survival and **C.** hypertension free survival are greater for participants with high structural versus high load-dependent stiffness.

Poster #39

Role Af a/b-Hydrolase Domain 2 (ABHD2) In Lipid Metabolism

Tara R. Price[1], Kathryn Schueler[1], Mark Keller[1], Alan Attie[1]

[1]*Department of Biochemistry, University of Wisconsin-Madison*

Background: ABHD2 is a novel lipase in the a/b hydrolase domain (ABHD) family of enzymes. While other members of the ABHD family, (ABHD6, ABHD12 and ABHD17) have been well characterized for their role in lipid metabolism, the substrates of ABHD2 have not been identified. Through integration of hepatic gene expression and lipidomics from ~500 Diversity Outbred mice fed a western-style diet for 4 months, our lab has mapped gene loci associated with the abundance of lipids in the serum and liver. In this study, we discovered that phosphatidylcholine (PC) maps to a locus containing the Abhd2 gene and increased hepatic *Abhd2* gene expression is associated with a decrease in hepatic PC.

We hypothesize the metabolic gene ABHD2 is a novel regulator of a broad class of lipids that includes PC in liver. As such, genetic regulation of lipids through the ABHD genes may play a key role in metabolic and cardiovascular disease development.

Methods: To explore the role of ABHD2 in lipid metabolism, I overexpressed *Abhd2* in HEK-293T cells. I identified two catalytic motifs in ABHD2: serine hydrolase and acyltransferase. I created two mutant plasmids which created a catalytically dead enzyme for each of these enzymatic sites and transfected HEK-293T cells with wild-type ABHD2 (WT-ABHD2), ABHD2 with a mutated serine hydrolase (mSH-ABHD2), or ABHD2 with a mutated acyltransferase motif (mAT-ABHD2). Untreated and GFP overexpressing HEK cells served as normal and vehicle controls. Cell pellets (n=3 technical replicates per treatment) were collected 48 hours post-transfection, snap frozen in liquid nitrogen, and submitted for untargeted lipidomics through the Advanced Lipidomics Platform (Biotechnology Center, University of Madison-Wisconsin).

Results: Wild-type ABHD2 (WT-ABHD2) overexpression showed a marked impact on lipid classes in the HEK-293T cells. PCs decreased with WT-ABHD2 overexpression, as predicted by the mouse genetic screen. There were also unexpected changes in other lipid classes, including ceramides and triglycerides. Through the mutant enzymes, I can also see trends in lipid classes that are altered through ABHD2's serine hydrolase activity, such as the long-chain PCs, and those that may be altered by the acyltransferase activity (CE:18:1, LPC 0:0/20:4).

Discussion: Until recently, hypertriglyceridemia was not recognized as a primary cause of cardiovascular disease and was instead thought to be a marker of low HDL. However, Mendelian randomization studies have now unequivocally shown that hypertriglyceridemia is a primary risk factor for CVD. Increased ABHD2 expression in HEK-293T cells reduced PC abundance, following the prediction by our genetic screens. Further analysis of changes in lipid classes showed that the decrease in PCs is associated with an increase in diglycerides, providing substrate for triglyceride formation. Thus, my work has uncovered a novel enzyme that affects a lipid strongly associated with CVD.

Poster #40

I_{K1} and β-2 Adrenergic Response: Implications For Caveolar Membranes

Louise Reilly[1], Kunal Sondhi[1], Hannah Waldman[1], Molly Melnick[1], Sara Abozeid[2], and Lee L. Eckhardt[1]

[1]Cellular and Molecular Research Program, Cardiovascular Research Center, University of Wisconsin - Madison
[2]Hematology and Oncology, Clinical Research Center, University of Wisconsin-Madison

Background: Cardiac remodeling in heart failure disrupts normal cellular structure and ion channel function resulting in risk for arrhythmic sudden death. I_{K1}, comprised dominantly of Kir2.1, is down-regulated in heart failure, resulting in decreased repolarization reserve. Heart failure has been shown to disrupt cellular micro-domains, caveolae, which coordinate ion channels and signaling molecules. As a result, ion channel function and intracellular signaling may be altered. Our previously published work revealed that Cav3 and Kir2.1 associate at the sarcolemma, intercalated discs and T-tubules. The effect of Cav3 on Kir2.1 β2AR adrenergic signaling has not been studied.

Methods: Isolated ventricular myocytes from C57/BL6J mice 8-weeks post-MI surgery were analyzed by voltage clamp using standard protocols. Whole heart lysates were analyzed by discontinuous sucrose gradient and western blot to isolate caveolar membranes using standard protocols. Sucrose gradient fractions were analyzed by co-immunoprecipitation and western blot using standard protocols.

Results: Baseline I_{K1} recorded from heart failure (HF) ventricular myocytes (VMs) showed decreased inward current at -100mV compared to sham VMs. Outward current at -50mV is decreased in VMs from HF mice compared to sham VMs. VMs were treated with 10μM atenolol followed by 10μM salbutamol. Response of outward and inward I_{K1} to atenolol and salbutamol was blunted in HF VMs compared to sham. Kir2.1 localized to caveolar domains, analyzed by discontinuous sucrose gradient, confirmed by the presence of caveolin-3. A small amount of β2AR localized to the same fractions. Interestingly, the majority of Kir2.1 and β2AR were found in fractions representing the bulk sarcolemma, suggesting that Kir2.1 co-localizes with β2AR outside of caveolae. Additionally, co-immunoprecipitation of pooled caveolar fractions (5-7) and bulk sarcolemmal fractions (8-12) revealed Kir2.1 and Cav3 associated in those fractions in both heart failure and sham.

Discussion: Heart failure results in downregulation of I_{K1} current and loss of I_{K1} β2-adrenergic sensitivity in cardiac cells compared to sham. However, I_{K1} and β2-adrenergic receptor downregulation appears independent of caveolar membrane disruption.

Homeostatic Control Of Cardiac Excitability By An RNA-Based Mechanism

Erick B. Ríos Pérez[1], Fang Liu[1], Gail A. Robertson[1]

Dept. of Neuroscience and Cardiovascular Research Center, University of Wisconsin School of Medicine and Public Health, 1111 Highland Ave. #5505, Madison, WI 53705, United States of America

Coordinated activity of ion channels in the human heart is essential for normal cardiac function and preventing life-threatening arrhythmias. We previously reported a cotranslational interaction between *KCNH2* and *SCN5A* transcripts respectively encoding the human *ERG* (hERG) potassium channel and Nav1.5 sodium channel. In addition to their association during biogenesis, these transcripts and the corresponding membrane currents are also subject to a curious co-knockdown effect elicited by selective RNAi of either transcript. Here, we hypothesized that simultaneous loss of the associated transcript serves a homeostatic role, preventing an imbalance of ion channels with opposing effects on membrane potential and action potential duration. To test this hypothesis, we plated human induced pluripotent stem cell-derived cardiomyocytes (iPSC-CMs) on a multielectrode array (MEA) platform in which electrophysiological activity could be measured from a monolayer syncytium as a proxy for cardiac tissue. Pharmacological block of hERG ion channels by dofetilide at IC_{50} concentrations predictably prolonged the action potential duration and increased the beat-to-beat variability, both cellular substrates for pro-arrhythmia. In contrast, viral transduction of a hERG-specific shRNA only modestly perturbed physiological function despite reduction of hERG mRNA by ~60% as assayed by qPCR. We infer that a compensatory effect was afforded by the concomitant knockdown of *SCN5A* mRNA levels, which showed quantitatively similar reductions. In separate experiments using patch clamp of isolated cells, I_{Kr} and I_{Na} amplitudes were also reduced by about half. RNAi-treated cells perfused with dofetilide showed less field potential prolongation compared to control cells, consistent with a reduced number of functional hERG channels after silencing. Thus, the balance of hERG and Nav1.5 protein is maintained after silencing one species of mRNA, suggesting a homeostatic coregulation by an RNA-based mechanism during biogenesis. Supported by NIH/NHLBI R01HL131403 (GAR).

Poster #42

Human Cardiac Fibroblasts Transition To Myofibroblasts *In Vitro* And Differentially Express Angiogenic And Inflammatory Cytokines

Sushmita Roy[1], Tianhua Zhou[1], Eric G. Schmuck[1], Amish N. Raval[1,2]

[1] Division of Cardiovascular Medicine, Department of Medicine, University of Wisconsin School of Medicine and Public Health, Madison, WI, USA.
[2]Department of Biomedical Engineering, University of Wisconsin, Madison, WI, USA.

Background: Cardiac fibroblasts (CFs) are the cells of the heart primarily responsible for the production and maintenance of extracellular matrix (ECM). Following injury, CFs differentiate into cardiac myofibroblasts (CMFs). CMFs produce copious amounts of collagen rich ECM to stabilize the damaged tissue, ultimately forming a dense, non-contractile scar. While the role of CMFs in scar formation is well documented, less is understood about the role of CFs and CMFs in resolving post infarction inflammation and angiogenesis. In this study, we tested the hypothesis that a transition from CF to CMF results in a reduction in inflammatory cytokine and an increase in angiogenic cytokines.

Methods: Human CFs (n=6, 3 male and 3 female) were isolated from healthy donor hearts that went unused for transplant and cultured in growth media (MCDB131+ 10% fetal bovine serum, 1 ng/ml FGF, 5 mg/ml insulin, 10 µg/ml ciproflaxin and 2.5 mg/ml amphotericin B). Flow cytometry was used to phenotype the CFs, markers included CD73, CD90, CD105, SUSD2, PDGFR and Periostin. The CMF marker periostin was used to confirm CF differentiation. Passage 1 (P1) CFs were plated into T75 flasks at a density of $1x10^6$ cells per flask in growth media. After 24 hours, the growth media was removed and stored for cytokine analysis. At passage 3 (P3), the CFs were plated in fresh growth media, after 24 hours, the media was removed and stored for cytokine analysis and flow cytometry was used to phenotype the cells as described above. Secretome analysis: 36 analytes were analyzed using the LEGENDplex™ (BioLegend) Human Inflammation panel 1 and 2 (catalog # 740809 and 740776) and human angiogenesis panel (catalog # 740698) and were carried out according to manufactures' protocols. Data analysis was carried out using the LEGENDplex™ Data Analysis Software to quantify the analyte concentrations in each sample.

Results: CFs at passage 1 expressed the following markers, CD73 (99.4 ± 0.43%), CD90 (31.2 ± 0.30%), CD105 (90.5± 4.5%), PDGFR (99.6 ± 0.03%) and SUSD2 (98.8 ± 0.03%). Periostin expression at passage 1 was 31.8 ± 0.4% and an MFI of 407 ± 16, confirming a primarily CF phenotype. At passage 3, periostin expression increased to 99.6 ± 0.1% and an MFI of 45,095 ± 219 confirming a shift to a primarily CMF phenotype. With increased periostin expression we observed a significant increase in angiogenic cytokines, the change in (delta) expression of the cytokines from P3 to P1 are listed: IL-6 (8095 ± 1220 pg/ml), Ang-2 (1070 ± 413 pg/ml), b-FGF (22.8 ± 5.8 pg/ml) and VEGF (1028 ± 285 pg/ml). Conversely, inflammatory cytokines including IFN gamma (-14 ± 1.3 pg/ml), TNF-alpha (-0.72 ± 0.12 pg/ml), IL-8 (-1408 ± 227 pg/ml), TGB-1 (-233 ± 22.7 pg/ml), sTREM-1 (-55 ± 7.16 pg/ml), and sRAGE (-285 ± 40.5 pg/ml) were reduced with increased periostin expression, CMF differentiation, *in vitro*.

Discussion: Until recently, the role of CFs in cardiac healing was thought to be limited to scar formation and post injury fibrosis. Here we demonstrate that CFs, by transitioning to a CMF, up regulate angiogenic cytokines while down regulating inflammatory cytokines indicating that CMFs may have an important role in the resolution of inflammation by suppression of inflammatory cytokines and increasing in cardiac vascularity post injury by increased angiogenic cytokine upregulation.

Whole-Cell Mechanical Loading And Unloading Triggers More Post-Translational Modifications In Z-disc Proteins Than Myosin Activators And Inhibitors

Christopher Solís, Elisabeth DiNello, Chad M. Warren, Kyle Dittloff, R. John Solaro, and Brenda Russell

Department of Physiology and Biophysics, University of Illinois at Chicago, Chicago, IL 60612

Background: The hypothesis tested is that unloading of mechanical forces affects acetylation, ubiquitination and phosphorylation of α-actinin and CapZ, which are actin-binding proteins in the Z-disc.

Methods: We applied targeted proteomics to interrogate the post-translational modification changes during loading and unloading. Cell morphology and post-translational modifications were determined in a mechanical intervention consisting of 1 Hz cyclic strain for 24 hr (loaded) followed by 6 hr rest (unloaded) of cultured neonatal rat ventricular myocytes (NRVMs). This was compared to a chemical intervention consisting of treating NRVMs with the myosin inhibitor Mavacamten (1 μM, 6hr) or Omecamtiv Mecarbil (0.5 μM, 6hr).

Results: Quantitative immunofluorescence showed both chemical and mechanical loading increase α-actinin content while Mavacamten decreased the α-actinin content. Affinity purification of α-actinin and CapZ and mass spectrometry analysis revealed that the mechanical intervention led to increased levels of post-translational modifications compared with the chemical interventions. Specifically, α-actinin ubiquitination increased with mechanical loading-unloading; acetylation decreased with mechanical loading-unloading and increased with mechanical loading; and phosphorylation remained unchanged with mechanical loading-unloading but increased with mechanical loading. Fluorescence recovery after photobleaching (FRAP) experiments demonstrated that Mavacamten increased the dynamics of a YFP-tagged α-actinin and a GFP-tagged CapZ expressed in NRVMs when compared to Omecamtiv Mecarbil treatments and controls.

Discussion: Overall, the results suggest a link between sarcomere homeostasis and mechanical forces via mechanisms involving acetylation, phosphorylation and ubiquitination of α-actinin and CapZ. These findings could have consequences for cardiac heart disease with abnormal sarcomeric proteostasis. Funded by NIH grants HL151825 (CS) and HL62426 (RJS, BR, and CMW).

Poster #44

Persistent Asthma Is Associated With Carotid Plaque In The Multi-Ethnic Study Of Atherosclerosis (MESA)

Matthew C. Tattersall[1], Alison Dasiewicz[2], Robyn L. McClelland[2], Claudia E. Korcarz[1], Stephane Esnault[3], Moyses Szklo[4], Nizar N. Jarjour[3], James H. Stein[1]

[1] Division of Cardiovascular Medicine, Department of Medicine, UWSMPH
[2]Collaborative Health Studies Coordinating Center, University of Washington, Seattle, WA
[3] Division of Allergy, Pulmonary and Critical Care Medicine, Department of Medicine, UWSMPH
[4]Department of Epidemiology, Johns Hopkins University, Baltimore, MD, United States

Background: Asthma and cardiovascular disease (CVD) share an underlying inflammatory pathophysiology. We hypothesized that persistent asthma is associated with carotid plaque burden, a strong predictor of future CVD events, and that this association would remain significant after adjustment for baseline inflammatory markers.

Methods: The Multi-Ethnic Study of Atherosclerosis is a cohort study of 6,814 adults free of CVD at baseline (Exam 1). Presence and severity of asthma was determined at Exam 1 as self-reported physician diagnosed. Persistent asthma was defined as asthma requiring use of controller medications (inhaled/oral corticosteroids, leukotriene inhibitors). Intermittent asthma was defined as asthma without use of controller medications. B-mode carotid ultrasound was performed at Exam 1, carotid plaque presence and score (range 0-12) were measured. Multivariable logistic and linear regression modeling with robust variances were used to assess the association of asthma subtype and carotid plaque.

Results: The 5,029 participants with complete data were a mean (standard deviation) 61.6 (10.0) years old (53% female, 26% African-American, 23% Hispanic, 12% Chinese). Carotid plaque was present in 50.5% of the non-asthmatics (N=4,532) with a mean±SD total plaque score of 1.29±1.8; 49.5% of intermittent asthmatics (N=388) with total plaque score of 1.25±1.76 and 67% of persistent asthmatics (N=109) with a total plaque score of 2.08±2.35 (all $p \leq 0.003$). In models adjusted for demographic and CVD risk factors, persistent asthma was associated with carotid plaque presence (odds ratio [OR], 1.83 [95% CI, 1.21-2.76], $p<0.001$), and carotid plaque score ($\beta=0.65$, $p<0.01$). The association of persistent asthma and carotid plaque remained significant after adjustment for baseline IL-6 (OR [95% confidence interval] 1.65 [1.08-2.51], $p=0.02$) or C-reactive protein (OR 1.77 [1.17-2.70], $p=0.01$) (Figure).

Conclusions: In a large multiethnic cohort, persistent asthma, but not intermittent asthma, was associated with carotid plaque presence and burden. These associations remained significant after adjustment for baseline inflammatory biomarkers

A Synthetic Biology Approach To Study Per-Arnt-Sim (PAS) Proteins In Cardiovascular Biology And Disease.

Alex C. Veith[1,2], Brenda Rojas[1,3], Emmanuel Vasquez-Rivera[1,3,4], Christopher A. Bradfield[1,2,3,4]

[1]McArdle Laboratory for Cancer Research,
[2]Cardiovascular Research Center,
[3]Molecular and Environmental Toxicology, University of Wisconsin School of Medicine and Public Health, Madison, WI 53706
[4]Biotechnology Center, University of Wisconsin-Madison, Madison, WI 53706

Background: The Per-Arnt-Sim (PAS) superfamily of proteins are a diverse group of environmental sensors that regulate responses to a variety of stimuli, including the microbiome, oxygen concentration, and circadian rhythms. Several PAS domain containing proteins have well established roles in cardiovascular biology, including the hypoxia inducible factors (HIFs) and KCNH channels. Further, our laboratory has shown that the aryl hydrocarbon receptor (AHR) plays an important role in hepatovascular development. Many of the PAS proteins in mammals are nuclear transcriptional regulators, such as HIF-1α, AHR, CLOCK and PER, and are known to have homo- and hetero-dimer formation through direct PAS domain interactions. While the KCNH channels have PAS domains, to the best of our knowledge, there is little evidence to show that these PAS domains interact with PAS domains of other proteins. A major goal of this research is to understand the biological role of PAS domains of the KCNH channels, and examine their potential to influence physiology with known nuclear PAS member. Such information may shed insight into causes of cardiac arrhythmias and sudden death.

Methods: To address this, we propose to utilize precision genome engineering and synthetic biology in *Saccharomyces cerevisiae* in conjunction with classic approaches, such as yeast two-hybrid. We propose to fuse the PAS domain of the KCNH channels to the LexA DNA binding protein as the bait while we screen full-length PAS proteins as the prey. In parallel, we will employ the CNBH domain fused to an activation domain as a positive control. If the bait and prey proteins interact, they will drive the expression of a reporter gene, LacZ. To increase the flexibility of this system and to allow future modifier screens, we propose to generate this model using CRISPR-Cas9 technology. The utility of the CRISPR-Cas9 in *S. cerevisiae* is that yeast readily use homologous recombination to repair DNA breaks, leading to high integrative transformation efficiency.

Results: We have previously used yeast two-hybrid approaches to show PAS-PAS interactions in yeast, and are currently creating the required recombinant strains for this study. We have also successfully integrated several required genes and a reporter into the yeast genome.

Discussion: Our group has previously shown the utility of *S. cerevisiae* in evaluating PAS protein interactions. Our goal is to use this system to evaluate the potential for any interaction between the PAS domains of the KCNH channels with PAS domains of other mammalian PAS proteins. We believe that incorporating CRISRP-Cas9 into our yeast two-hybrid approaches may allow us to include potential cofactors or modifiers that are needed for or enhance any interactions. These experiments will supplement other approaches we are using to study PAS protein interactions and DNA binding of nuclear receptor PAS proteins. Further, these experiments and approaches will complement other experiments design to discover novel alleles of other PAS proteins and study their role in cardiovascular biology disease.

Molecular And Cellular Characterization Of RyR2 Mutations Linked To Long-QT Syndrome

Wenxuan Cai[1,2], Talia Booher[1], Songhua Li[3], Jingjing Zheng[1], Francisco Alvarado[1,3], Teresa Villareal[4], Norma Balderabano[5], Argelia Mereidos-Domingo[6,7], Pedro Iturralde[8], Héctor H. Valdivia[1,3], Carmen R.Valdivia[1,3]

[1]Cardiovascular Research Center, University of Wisconsin-Madison, USA. [2]School of Pharmacy, University of Wisconsin-Madison, USA. [3]Department of Medicine, University of Wisconsin-Madison, USA. [4]Instituto Nacional de Medicina Genomica (INMEGEN) (The National Institute of Genomic Medicine), National Autonomous University of Mexico, Mexico. [5] Children's Hospital, Federico Gómez, Mexico City, Mexico. [6] Clinic for Cardiology, University Hospital Zurich, Switzerland. [7] Swiss DNAlysis, Switzerland. [8]National Institute of Cardiology, Ignacio Chavez, Mexico

Background: Long-QT syndrome (LQTS) is a cardiac disorder characterized by prolonged QT interval and abnormal T waves on electrocardiogram of the patients. Electrical abnormality of the heart can lead to severe arrhythmias, syncope and sudden cardiac death. Mutations in genes encoding the sodium and potassium channels or associated proteins account for approximately 80% of all cases; however, the genetic causes of the remaining 20% cases are poorly understood. Recent genetic studies revealed novel LQTS-associated variants on the cardiac ryanodine receptor (RyR2), a calcium channel localized in the sarcoplasmic reticulum membrane and largely responsible for calcium-induced calcium release and excitation-contraction coupling. Given the important roles of RyR2 in the electrical activity of cardiomyocytes and previous evidence of RyR2 mutations in other inherited arrhythmias, we hypothesized that RyR2 mutations lead to functional alterations of the channels and contribute to dysregulated calcium release and pathological electrical remodeling.

Methods: RyR2 mutations were generated using site-directed mutagenesis and expressed in HEK293 cells. [^{3}H] ryanodine binding assay was used to measure the opening probability of the RyR2 channels. HEK293 with stable expression RyR2 mutants were used to investigate luminal Ca2+ sensitivities of the channels. A mouse model was generated to investigate the membrane potential and calcium signaling alterations caused by RyR2 mutation.

Results and Discussion: In this study, we first characterized the intrinsic properties of RyR2 channels harboring ten novel mutations linked to LQTS in patients, including S166C, H877P, R1760W, G2094S, R2824W, R2920Q, R3673W, Y4287N, V4298M, P4534S and K4594Q. The [^{3}H] ryanodine binding assays revealed that LQTS-associated mutations had variable effects on the opening probability of the channel. Some mutations caused an increased channel opening, some reduced channel opening and some were indistinguishable from the WT in terms of opening probability. Using the stable cell lines, we measured the store-overload-induced Ca2+ release (SOICR), and showed that the LQTS-associated RyR2 mutations caused an increase in the luminal calcium sensitivity of the channel at various calcium concentrations. A transgenic mouse model carrying the R2920Q mutation was used to investigate the cellular phenotypes of the RyR2 mutation and elucidate the molecular pathways leading to LQTS. Homozygous mice showed prolonged QT intervals and QTc at 6 months, and electrophysiological studies revealed a depolarized resting membrane potential in the homozygous R2920Q cardiomyocytes compared to WT cells. Additionally, significant prolongation in action potential duration was observed in the mutation cardiomyocytes.

Future investigations on the effects of RyR2 mutations on the post-translational modifications of the channel and changes in the intracellular Ca2+-dependent signaling pathways will allow for further elucidation of the role of RyR2 in LQTS.

Differences In Clinical Characteristics And Risk of Death Between Recovered And Preserved Ejection Fraction Heart Failure

Nathan Wheeler, MD; Furqan Rajput, MD; Naga Dharmavaran, MD; Timothy Hess, PhD; Aurangzeb Baber, MD; Farhan Raza, MD; Ravi Dhingra MD, MPH

Division of Cardiovascular Medicine, Department of Medicine, University of Wisconsin-Madison.

Background: Heart failure patients with recovered left ventricular ejection fraction (HFrecEF) i.e. LVEF >40% have distinct pathophysiology compared to those with preserved ejection (HFpEF); however differences in clinical characteristics and outcomes of these patients remain unclear.

We hypothesized that patients with HFpEF when compared with HFrecEF have higher prevalence of comorbidities and greater risk of overall mortality.

Methods: We queried our health system and identified patients with LVEF <40% who then recovered and sustained their LVEF to>40% from 2009-2018 (n=705) and propensity-matched based upon age and gender to HFpEF patients (LVEF >50%; n=3525) in 1:5 ratio. Kaplan Meier curves and multivariate Cox models compared the risk of death between two groups.

Results: At the time of first encounter, HFpEF patients were more likely to have diabetes, hypertension, chronic kidney disease, pulmonary hypertension, and cancers (p value for all< 0.05). On follow up (mean 3.3 years), 1053 patients died. Kaplan Meier curves showed HFpEF patients to have increased risk of death when compared to HFrecEF patients (Figure). Multivariable Cox models also showed higher risk of death in HFpEF patients compared to HFrecEF patients (Hazard Ratio 1.71, 95% CI 1.41 –2.08; p<0.0001).

Conclusions: HFpEF patients have significantly higher prevalence of comorbidities and greater risk of death compared to the HFrecEF patients. Further research to examine causal pathways of developing HFpEF and reducing mortality are warranted.

Heart Field-Specific Lineages Differentiated From Human Pluripotent Stem Cells Generate Chamber-Specific Cardiomyocytes For Disease Modeling And Cell Therapies

Jianhua Zhang[1,2], Gina Kim[1], Peng Zhao[3], Reza Ardehali[3], Tim Kamp[1, 2, 4]

[1]Department of Medicine
[2]Stem Cell and Regenerative Medicine Center
[3]Department of Internal Medicine, University of California, Los Angeles
[4]Department of Cell and Regenerative Biology

Background: Adult heart consists of chamber-specific cardiomyocytes (CMs) derived from two major populations of mesodermal progenitors, first heart field (FHF) and second heart field (SHF). FHF-derived CMs contribute to left ventricle (LV), while SHF-derived CMs form right ventricle (RV) and outflow tract, and both FHF- and SHF-derived atrial CMs contribute to atria. Certain forms of inherited heart disease impact chamber-specific CMs such as arrhythmogenic right ventricular cardiomyopathy (ARVC) and Brugada Syndrome which primarily impact the RV and right ventricular outflow track. Other pathology can impact specifically the atria such as atrial fibrillation. The primary functional abnormality for many dilated cardiomyopathies is often in LV CMs. Thus, to use human pluripotent stem cell-derived CMs (hPSC-CMs) to investigate the disease mechanisms, toxicities, and treatment strategies ideally requires the appropriate chamber-specific CMs. We hypothesize that hPSCs can be differentiated to FHF and SHF progenitors from which the subtypes of CMs that contribute to LV, RV and atria can be derived and used for different forms of cardiac disease modeling and cardiac repair and regeneration.

Methods: A genetically engineered human embryonic stem cell (hESC) reporter line, hES3-*TBX5*$^{TdTomato/W}$/*NKX2-5*$^{eGFP/W}$, and a normal hiPSC line DF19-9-11T are used in this study. The hESC reporter line utilizes two important transcription factors in cardiac development, NKX2-5 and TBX5, whose combination of expression enables recognition and isolation of FHF and SHF progenitors and their derived CMs. Three monolayer-based differentiation protocols were developed by modulation of canonical Wnt, FGF, BMP and noncanonical Wnt signaling to direct hPSCs to differentiate to FHF and SHF progenitors and their derived LV- and RV-CMs as well as using retinoic acid (RA) signaling to promote atrial CMs differentiation. Flow cytometry were used to identify FHF and SHF progenitors by combination of NKX2-5-eGFP and TBX5-TdTomato expressing cells, as well as CMs by labeling the cells with cTnT antibody and analyzing with NKX2-5-eGFP and TBX5-TdTomato concurrently.

Results: The differentiation protocol by modulation of canonical Wnt signaling showed NKX2-5$^+$/TBX5$^+$ cells indicate FHF progenitors differentiated in the early stage (day 6-9). Continuous differentiation of the FHF progenitors generated CMs (cTnT$^+$) with the majority expressing NKX2-5 and TBX5. The differentiation protocol by upregulation of canonical Wnt and FGF signaling followed by BMP and noncanonical Wnt signaling promoted differentiation of SHF progenitors which are NKX2-5$^+$/TBX5$^-$ cells and generated cTnT$^+$ CMs with the majority being NKX2-5$^+$ but TBX5$^-$, indicating SHF-lineage of RV and outflow tract CMs. RA signaling when applied in the early time window of differentiation in both protocols (day 5-9 and day 2.75-5, respectively) can promote formation of atrial-like CMs marked by the expression of NR2F2. qRT-PCR of FHF and SHF transcription factors as well as ventricular and atrial CM markers confirmed the FHF- and SHF-lineage specific gene expression.

Discussion: The FHF- and SHF-lineages can be differentiated using different protocols by dynamically modulating growth factor signaling. The FHF- and SHF-lineages were identified by flow cytometry, gene expression and immunolabeling for specific markers expression. Future studies will characterize the CMs by their electrophysiological properties. Chamber-specific CMs will advance the ability to model both inherited and acquired heart diseases as well as generate improved cell therapy products.

Poster #49

Cultured Human Cardiac Myofibroblast's Expression Of Sushi Containing Domain 2 Predicts The Assembly Of Intact Fibronectin-Rich Extracellular Matrix

Tianhua Zhou[1], Sushmita Roy[1], Eric Schmuck[1], James Conklin[2], Nisha Wattanayuth[2], Deane Mosher[3], Jean Schwarzbauer[4], Amish Raval[1,2]

[1]Division of Cardiovascular Medicine, Department of Medicine, University of Wisconsin School of Medicine and Public Health, Madison, WI, USA
[2]Department of Biomedical Engineering, University of Wisconsin, Madison, WI, USA
[3]Department of Biomolecular Chemistry, University of Wisconsin, Madison, WI, USA
[4]Department of Molecular Biology, Princeton University, Princeton, NJ, USA

Introduction: Fibronectin (FN) has key roles in cell adhesion, differentiation, migration, alignment and immune modulation in the developing heart, but is of low abundance in the postnatal heart. Replenishing injured myocardium with insoluble FN could be a novel therapeutic approach; however, methods to produce an ECM rich in insoluble FN have remained elusive. Our team developed a method to produce decellularized fibronectin-rich (dFN) sheets assembled by dense human cardiac myofibroblast (CMF) cultures. We discovered that the transmembrane protein, Sushi Containing Domain 2 (SUSD2), is broadly expressed on cultured CMFs. We hypothesized that SUSD2 abundance predicts whether CMFs produce intact dFN sheets.

Methods: Primary CMFs were isolated from healthy left ventricle of human cadaveric donors. CMFs were sorted by median fluorescence intensity (MFI) into $SUSD2^{Bright}$ and $SUSD2^{Dim}$ CMF populations using flow cytometry. Methods to produce dFN sheets were applied to both populations, and the resulting ECM was graded: 0=no ECM 1=fragmented, 2=friable and 3=intact sheet (Figure).

Results: SUSD2 was detected on 98±1% of CMFs among 7 strains. The average MFI ($x10^3$) was 167±51. CMF strains that produced Grade 0-2 (n=4) and Grade 3 (n=3) dFN sheets had an average MFI of 62 and 270, respectively (P=<0.001). $SUSD2^{Bright}$ cells sorted from natural $SUSD2^{Dimer}$ strains produced intact sheets. Conversely, $SUSD2^{Dim}$ cells sorted from a natural $SUSD2^{Brighter}$ strains failed to produce intact sheets.

Conclusions: SUSD2 abundance on CMFs predicts intact dFN sheet production. Ongoing protein analyses of these sheets are expected to enhance our understanding of SUSD2's previously unidentified role in CMFs that drive cardiac ECM assembly.